Georgia Tech, June 12-22

Stochastic Methods in Robotics (Probability, Fourier Analysis, Lie Groups and Applications)

Gregory S. Chirikjian

Department of Mechanical Engineering
Johns Hopkins University

Contents

Binary Manipulators in Our Lab

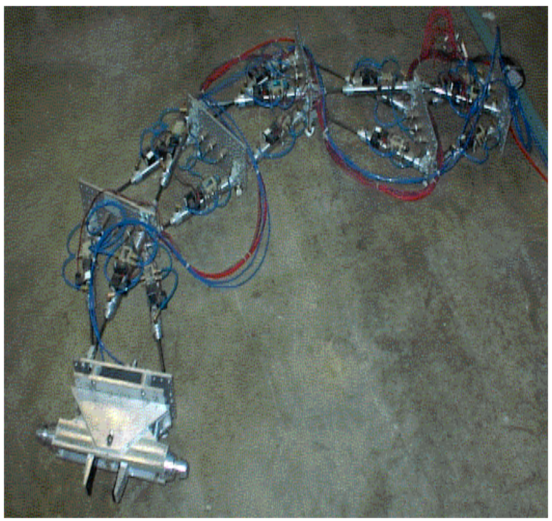

$2^{15} \approx 3.3\times10^{4}$ configurations

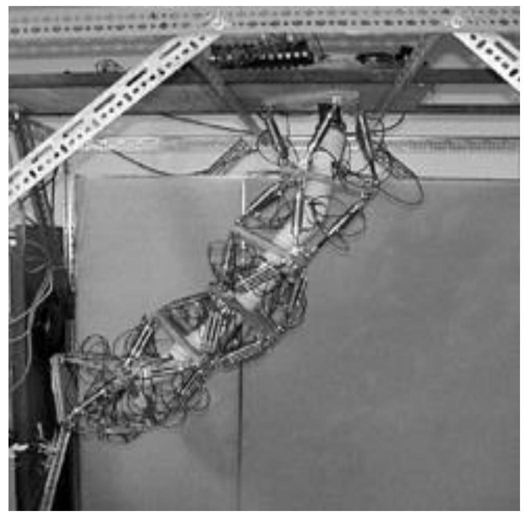

$2^{36} \approx 6.9\times10^{10}$ configurations

2.1×10^{6} configuration s

Workspace Density

- It describes the density of the reachable frames in the work space.
- It is a probabilistic measurement of accuracy over the workspace.

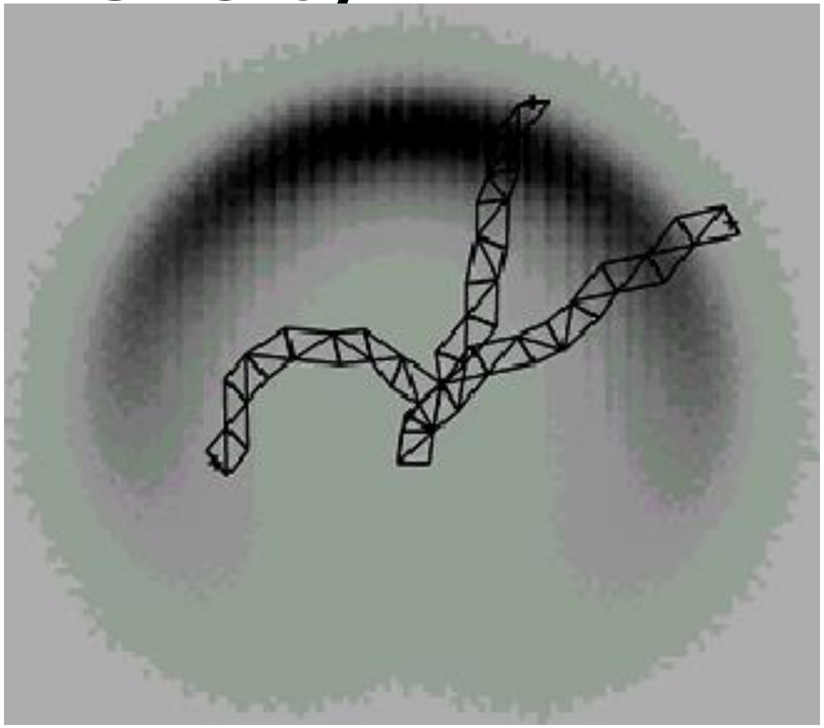

Ebert-Uphoff, I., Chirikjian, G.S., ``Inverse Kinematics of Discretely Actuated Hyper-Redundant Manipulators Using Workspace Densities,'' ICRA'96, pp. 139-145

Long, A.W., Wolfe, K.C., Mashner, M.J., Chirikjian, G.S., ``The Banana Distribution is Gaussian: A Localization Study with Exponential Coordinates,'' RSS, Sydney, NSW, Australia, July 09 - July 13, 2012.

SDE for the Kinematic Cart

(Zhou and Chirikjian, ICRA 2003)

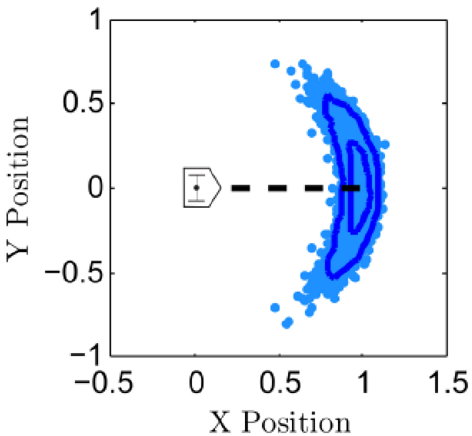

(a)

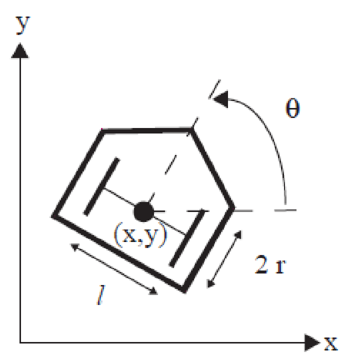

(b)

$$\begin{pmatrix} dx \\ dy \\ d\theta \end{pmatrix} = \begin{pmatrix} \frac{r}{2}(\omega_1 + \omega_2)\cos\theta \\ \frac{r}{2}(\omega_1 + \omega_2)\sin\theta \\ \frac{r}{\ell}(\omega_1 - \omega_2) \end{pmatrix} dt + \sqrt{D} \begin{pmatrix} \frac{r}{2}\cos\theta & \frac{r}{2}\cos\theta \\ \frac{r}{2}\sin\theta & \frac{r}{2}\sin\theta \\ \frac{r}{\ell} & -\frac{r}{\ell} \end{pmatrix} \begin{pmatrix} dw_1 \\ dw_2 \end{pmatrix}$$

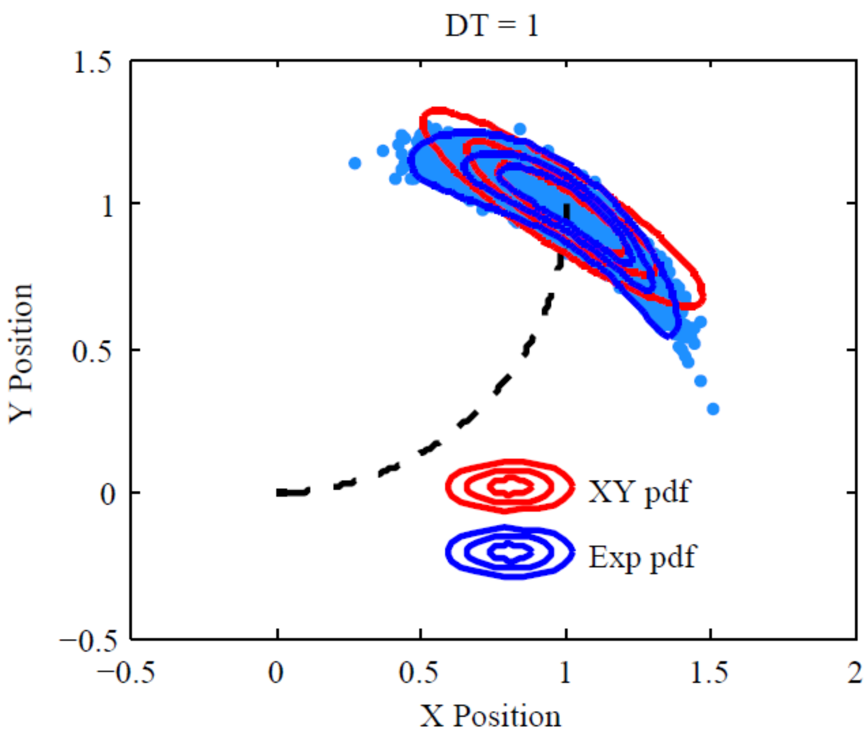

A. Long, K. Wolfe, M. Mashner, G. Chirikjian, ``The Banana Distribution is Gaussian” RSS 2012

$$\int_G \log^\vee \left(\mu^{-1} \circ g\right) f(g)dg = \mathbf{0}$$

$$\Sigma = \int_G \log^\vee(\mu^{-1} \circ g)[\log^\vee(\mu^{-1} \circ g)]^T f(g)dg$$

$$f(g;\mu,\Sigma) = \frac{1}{c(\Sigma)} \exp\left[-\frac{1}{2}\mathbf{y}^T\Sigma^{-1}\mathbf{y}\right]$$

$$\mathbf{y} = \log(\mu^{-1} \circ g)^\vee$$

$$A^{ij} = A_i A_j^{-1}$$
$$B^{ij} = B_i^{-1} B_j$$
$$\Rightarrow \quad A^{ij} X = X B^{ij}$$

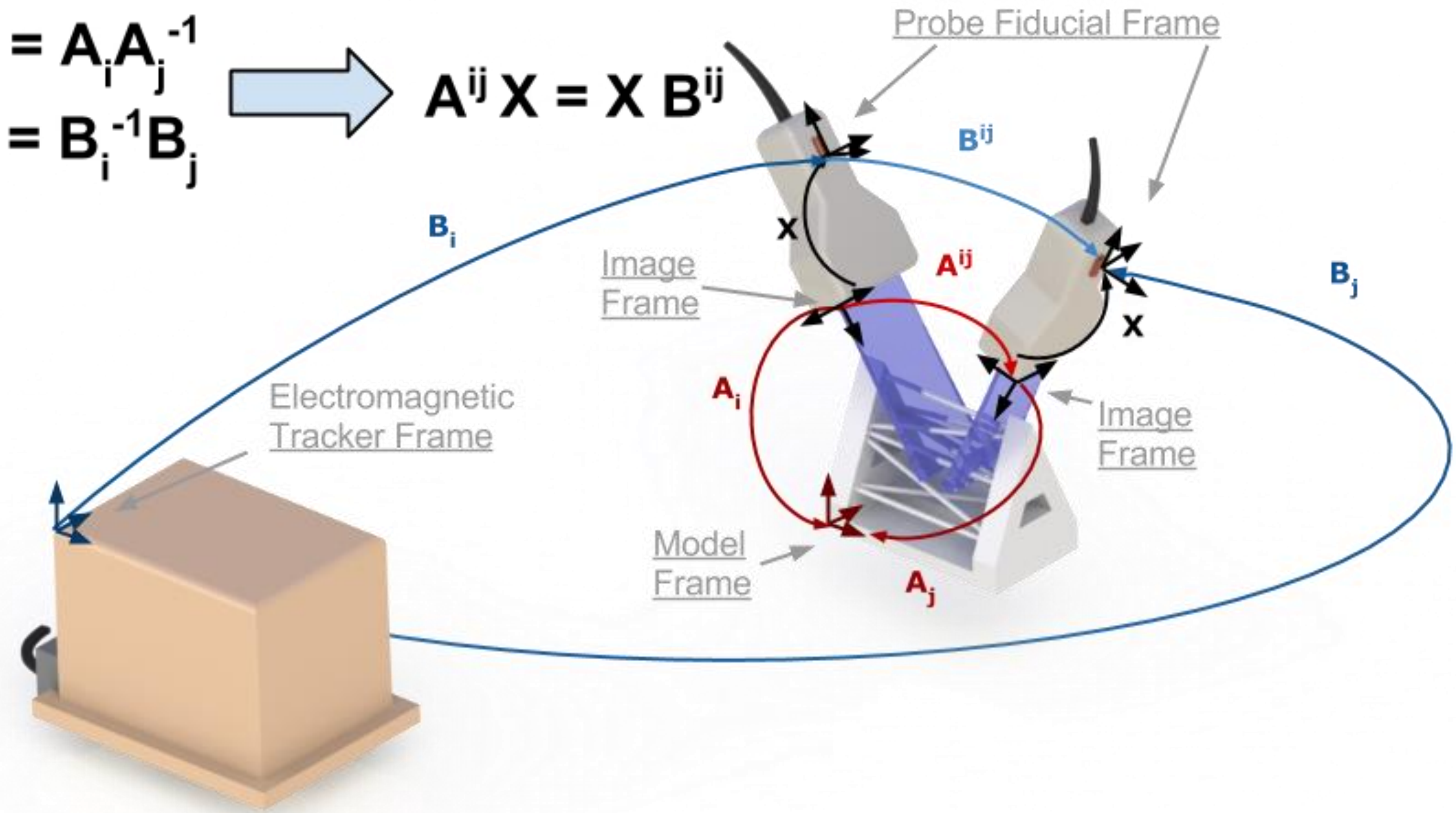

Examples of Lie Groups

$$GL(N,\mathbb{R}) \doteq \{A \in \mathbb{R}^{N\times N} \,|\, \det A \neq 0\}.$$

$$GL^{+}(N,\mathbb{R}) \doteq \{A \in GL(N,\mathbb{R}) \,|\, \det A > 0\}$$

$$SL(N,\mathbb{F}) \doteq \{A \in \mathbb{F}^{N\times N} \,|\, \det(A) = +1\} \subset GL(N,\mathbb{F})$$

$$U(N) \doteq \{A \in \mathbb{C}^{N\times N} \,|\, AA^{*} = \mathbb{I}\} < GL(N,\mathbb{C}).$$

$$SU(N) \doteq U(N) \cap SL(N,\mathbb{C}) < GL(N,\mathbb{C});$$

$$SO(N) \doteq \{A \in GL(N,\mathbb{R}) \,|\, AA^{T} = \mathbb{I};\ \det A = +1\} = U(N) \cap SL(N,\mathbb{R})$$

PART 1: INTRODUCTORY MATHEMATICS

PART 1(a): Probability and Statistics

Gaussian Distribution on the Real Line

$$\rho(x;\mu,\sigma^2) = \rho_{(\mu,\sigma^2)}(x) = \frac{1}{\sqrt{2\pi\sigma}} e^{-(x-\mu)^2/2\sigma^2}$$

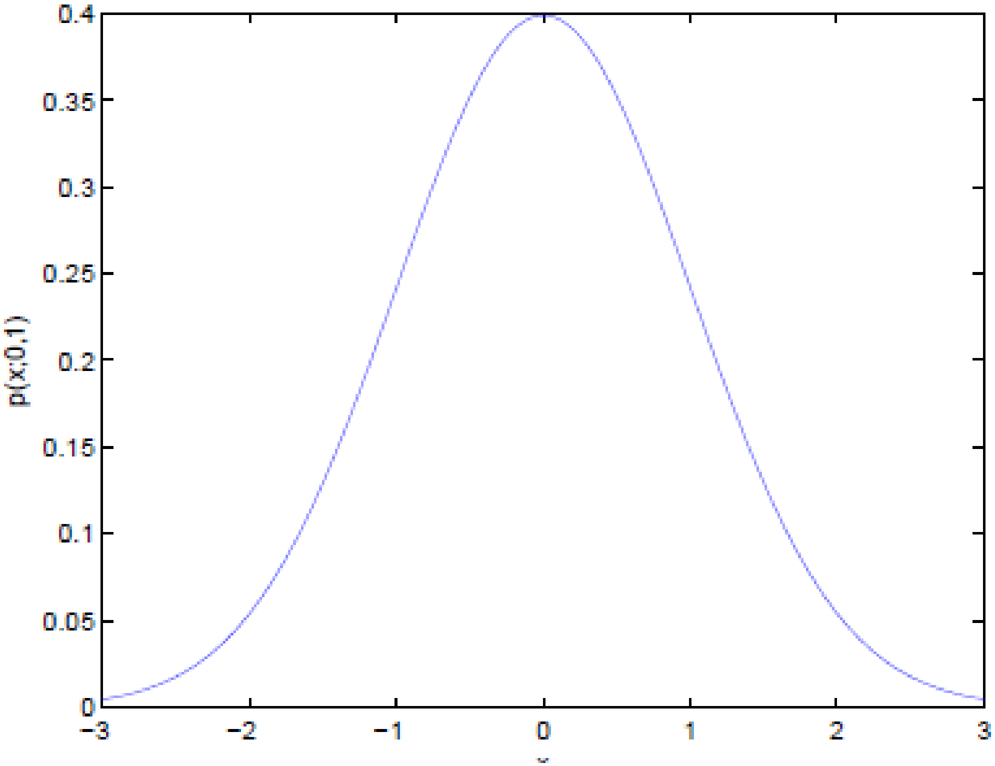

The Gaussian Distribution $\rho(x;0,1)$ Plotted over $[-3,3]$

Convolution of Gaussians

The *convolution* of two pdfs on the real line is defined as

$$(f_1 * f_2)(x) \doteq \int_{-\infty}^{\infty} f_1(\xi) f_2(x - \xi) d\xi.$$

It can be shown that the convolution integral will always exist for "nice" functions, and furthermore

$$f_i \in \mathcal{N}(\mathbb{R}) \implies f_1 * f_2 \in \mathcal{N}(\mathbb{R}).$$

The Gaussian distribution has the property that the convolution of two Gaussians is a Gaussian:

$$\rho(x; \mu_1, \sigma_1^2) * \rho(x; \mu_2, \sigma_2^2) = \rho(x; \mu_1 + \mu_2, \sigma_1^2 + \sigma_2^2)$$

The Dirac δ-function can be viewed as the limit

$$\delta(x) = \lim_{\sigma \to 0} \rho(x; 0, \sigma^2).$$

It then follows from (3.8) that

$$\rho(x; \mu_1, \sigma_1^2) * \delta(x) = \rho(x; \mu_1, \sigma_1^2).$$

Classical Fourier Analysis

The Fourier transform of a "nice" function $f \in \mathcal{N}(\mathbb{R})$ is defined as

$$[\mathcal{F}(f)](\omega) \doteq \int_{-\infty}^{\infty} f(x) e^{-i\omega x} dx.$$

The shorthand $\hat{f}(\omega) \doteq [\mathcal{F}(f)](\omega)$ will be used frequently.
From the definition of the Fourier transform, it can be shown that

$$(\widehat{f_1 * f_2})(\omega) = \hat{f}_1(\omega) \hat{f}_2(\omega)$$

$$f(x) = [\mathcal{F}^{-1}(\hat{f})](x) \doteq \frac{1}{2\pi} \int_{-\infty}^{\infty} \hat{f}(\omega) e^{i\omega x} d\omega.$$

Gaussians Wrapped Around the Circle

$$\rho_W(\theta;\mu,\sigma^2) \doteq \sum_{k=-\infty}^{\infty} \rho(\theta - 2\pi k;\mu,\sigma^2)$$

This is exactly equivalent to

$$\rho_W(\theta;\mu,\sigma^2) = \frac{1}{2\pi} + \frac{1}{\pi}\sum_{n=1}^{\infty} e^{-\frac{\sigma^2}{2}n^2}\cos\left(n(\theta-\mu)\right)$$

Gassian as Solution to Heat Equation (circle case)

$$\frac{\partial f}{\partial t} = \frac{1}{2} k \frac{\partial^2 f}{\partial \theta^2} \quad \text{subject to} \quad f(\theta, 0) = \delta(\theta)$$

$$f(\theta, t) = \sum_{k=-\infty}^{\infty} \rho(\theta - 2\pi k; 0, (kt)\ \ )$$

$$= \frac{1}{2\pi} + \frac{1}{\pi} \sum_{n=1}^{\infty} e^{-ktn^2/2} \cos n\theta$$

Gassian as Solution to Heat Equation (R^n case)

$$\frac{\partial f}{\partial t} = \frac{1}{2}\sum_{i,j=1}^{n} D_{ij}\frac{\partial f^2}{\partial x_i \partial x_j}$$

$$f(\mathrm{x}, t) = \frac{1}{(2\pi t)^{n/2}|\det D|^{\frac{1}{2}}}\exp(-\frac{1}{2t}\mathrm{x}^T D^{-1}\mathrm{x})$$

Multivariate Gaussian

$$\rho(\mathbf{x};\boldsymbol{\mu},\Sigma) \doteq \frac{1}{(2\pi)^{n/2}|\det\Sigma|^{\frac{1}{2}}}\exp\left\{-\frac{1}{2}(\mathbf{x}-\boldsymbol{\mu})^T\Sigma^{-1}(\mathbf{x}-\boldsymbol{\mu})\right\}$$

$$\int_{\mathbb{R}^n}\rho(\mathbf{x};\boldsymbol{\mu},\Sigma)\,d\mathbf{x} = 1$$

$$\int_{\mathbb{R}^n}\mathbf{x}\,\rho(\mathbf{x};\boldsymbol{\mu},\Sigma)\,d\mathbf{x} = \boldsymbol{\mu}$$

$$\int_{\mathbb{R}^n}(\mathbf{x}-\boldsymbol{\mu})(\mathbf{x}-\boldsymbol{\mu})^T\rho(\mathbf{x};\boldsymbol{\mu},\Sigma)\,d\mathbf{x} = \Sigma$$

Convolution on R^n

$$(\rho_1 * \rho_2)(\mathbf{x}) = \int_{\mathbb{R}^n} \rho_1(\boldsymbol{\xi})\rho_2(\mathbf{x} - \boldsymbol{\xi})\, d\boldsymbol{\xi}$$

$$\boldsymbol{\mu}_{1*2} = \boldsymbol{\mu}_1 + \boldsymbol{\mu}_2 \text{ and } \Sigma_{1*2} = \Sigma_1 + \Sigma_2$$

A Little Bit of Information Theory

Entropy

$$S(f) \doteq -\int_{\mathbf{x}} f(\mathbf{x}) \log f(\mathbf{x}) d\mathbf{x}$$

Kullback-Leibler Divergence

$$D_{KL}(f_1 \| f_2) \doteq \int_{\mathbb{R}^n} f_1(\mathbf{x}) \log \left(\frac{f_1(\mathbf{x})}{f_2(\mathbf{x})} \right) d\mathbf{x}$$

Entropy Power Inequality

$$N(p) = \exp(2S(p)/n)/2\pi e$$

$$N(p * q) \geq N(p) + N(q)$$

PART 1(b): Lie Groups and Lie Algebras

Rigid-Body Motion Group

- Special Euclidean motion group *SE(N)*
  - An element of G=*SE(N)*:

$$g = \begin{pmatrix} A & a \\ 0^T & 1 \end{pmatrix}$$

  - Group operation: matrix multiplication
- For example, an element of *SE(2)* in polar coordinates:

$$g(\phi, r, \theta) = \begin{pmatrix} \cos\phi & -\sin\phi & r\cos\theta \\ \sin\phi & \cos\phi & r\sin\theta \\ 0 & 0 & 1 \end{pmatrix}$$

- Lie algebra of *SE(2)*

$$\tilde{X}_1 = \begin{pmatrix} 0 & -1 & 0 \\ 1 & 0 & 0 \\ 0 & 0 & 0 \end{pmatrix} \qquad \tilde{X}_2 = \begin{pmatrix} 0 & 0 & 1 \\ 0 & 0 & 0 \\ 0 & 0 & 0 \end{pmatrix} \qquad \tilde{X}_3 = \begin{pmatrix} 0 & 0 & 0 \\ 0 & 0 & 1 \\ 0 & 0 & 0 \end{pmatrix}$$

- Lie algebra of *SE(3)*

$$\tilde{X}_1 = \begin{pmatrix} 0 & 0 & 0 & 0 \\ 0 & 0 & -1 & 0 \\ 0 & 1 & 0 & 0 \\ 0 & 0 & 0 & 0 \end{pmatrix} \qquad \tilde{X}_2 = \begin{pmatrix} 0 & 0 & 1 & 0 \\ 0 & 0 & 0 & 0 \\ -1 & 0 & 0 & 0 \\ 0 & 0 & 0 & 0 \end{pmatrix} \qquad \tilde{X}_3 = \begin{pmatrix} 0 & -1 & 0 & 0 \\ 1 & 0 & 0 & 0 \\ 0 & 0 & 0 & 0 \\ 0 & 0 & 0 & 0 \end{pmatrix}$$

$$\tilde{X}_4 = \begin{pmatrix} 0 & 0 & 0 & 1 \\ 0 & 0 & 0 & 0 \\ 0 & 0 & 0 & 0 \\ 0 & 0 & 0 & 0 \end{pmatrix} \qquad \tilde{X}_5 = \begin{pmatrix} 0 & 0 & 0 & 0 \\ 0 & 0 & 0 & 1 \\ 0 & 0 & 0 & 0 \\ 0 & 0 & 0 & 0 \end{pmatrix} \qquad \tilde{X}_6 = \begin{pmatrix} 0 & 0 & 0 & 0 \\ 0 & 0 & 0 & 0 \\ 0 & 0 & 0 & 1 \\ 0 & 0 & 0 & 0 \end{pmatrix}$$

- Infinitesimal motions

$$H_i(\varepsilon) = \exp(\varepsilon \tilde{X}_i) \approx I + \varepsilon \tilde{X}_i$$

A Little Bit of Lie Group Theory

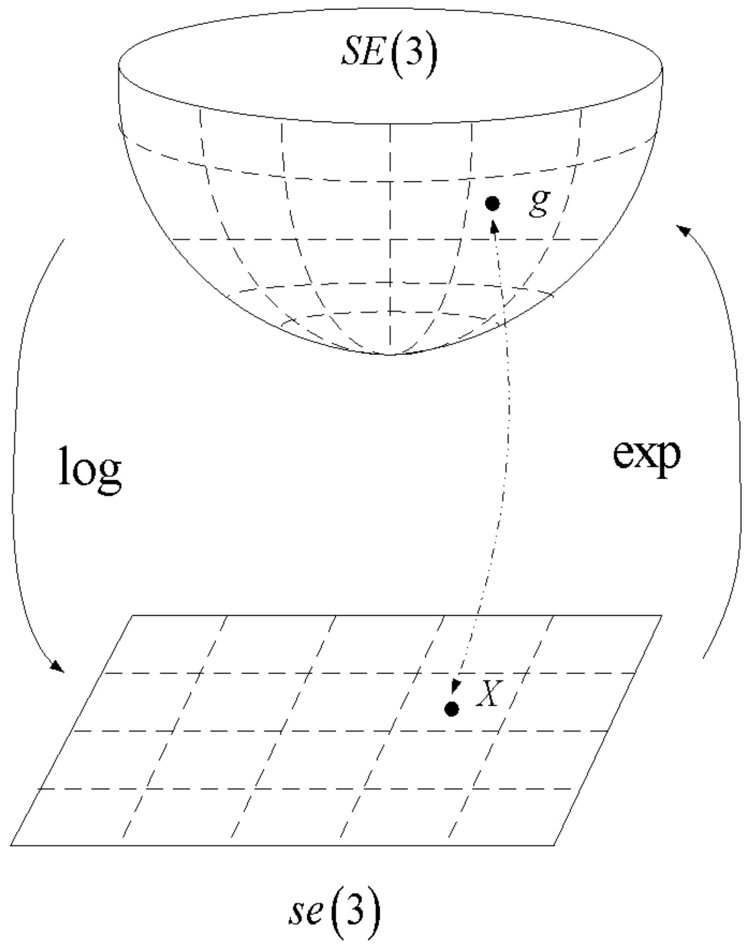

$$e^X = \mathbb{I} + \sum_{k=1}^{\infty} \frac{X^k}{k!}$$

exp and log for SO(3)

$$S = \begin{pmatrix} 0 & -s_3 & s_2 \\ s_3 & 0 & -s_1 \\ -s_2 & s_1 & 0 \end{pmatrix} \qquad S^\vee = \mathbf{s}, \qquad S\mathbf{x} = \mathbf{s} \times \mathbf{x}.$$

$$e^X = \mathbb{I} + \frac{\sin \|\mathbf{x}\|}{\|\mathbf{x}\|} X + \frac{(1 - \cos \|\mathbf{x}\|)}{\|\mathbf{x}\|^2} X^2$$

$$A(\mathbf{n}, \theta) = e^{\theta N} = \mathbb{I} + \sin\theta\, N + (1 - \cos\theta) N^2$$

$$\log(A) = \frac{1}{2} \frac{\theta(A)}{\sin\theta(A)} (A - A^T) \qquad \theta(A) = \cos^{-1}\left(\frac{\mathrm{trace}(A) - 1}{2}\right)$$

Lie-group-theoretic Notation

- Coordinate free $\rightarrow$ no singularities

For $A(t) \in SO(3)$,

$$A^T \dot{A} = \sum_{i=1}^{3} \omega_i X_i$$

$$\boldsymbol{\omega} = \left(A^T \dot{A}\right)^\vee$$

X_i : basis element of $so(3)$

For $g(t) = (\mathbf{a}(t), A(t)) \in SE(3)$

$$g^{-1}\dot{g} = \sum_{i=1}^{6} \xi_i X_i = \begin{pmatrix} A^T \dot{A} & A^T \mathbf{a} \\ \mathbf{0}^T & 0 \end{pmatrix}$$

$$\boldsymbol{\xi} = \left(g^{-1}\dot{g}\right)^\vee = \begin{pmatrix} \left(A^T \dot{A}\right)^\vee \\ A^T \dot{\mathbf{a}} \end{pmatrix} = \begin{pmatrix} \boldsymbol{\omega} \\ \mathbf{v} \end{pmatrix}$$

X_i : basis element of $se(3)$

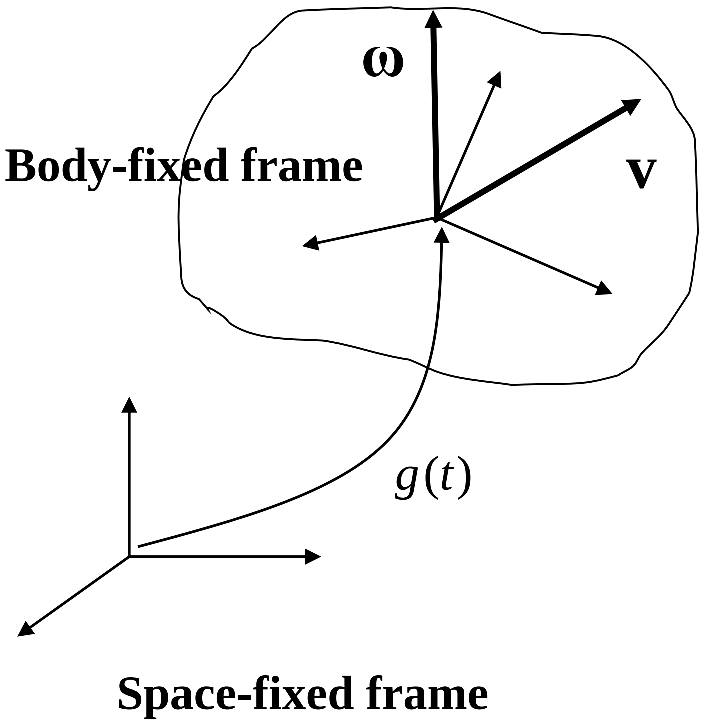

For more details see

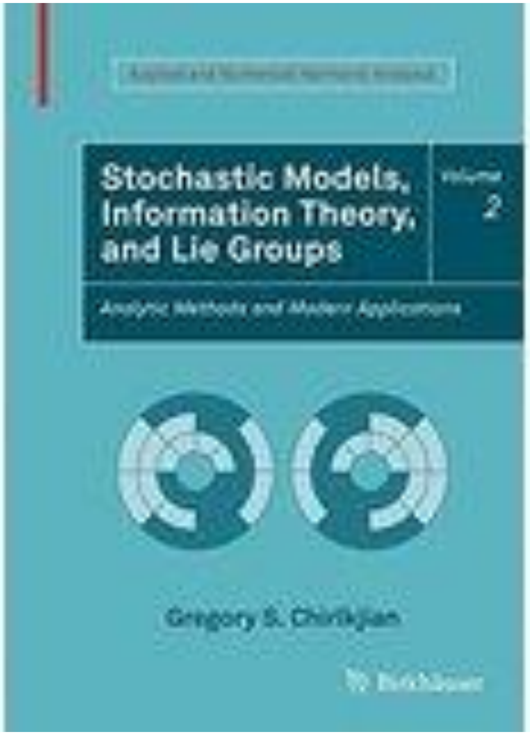

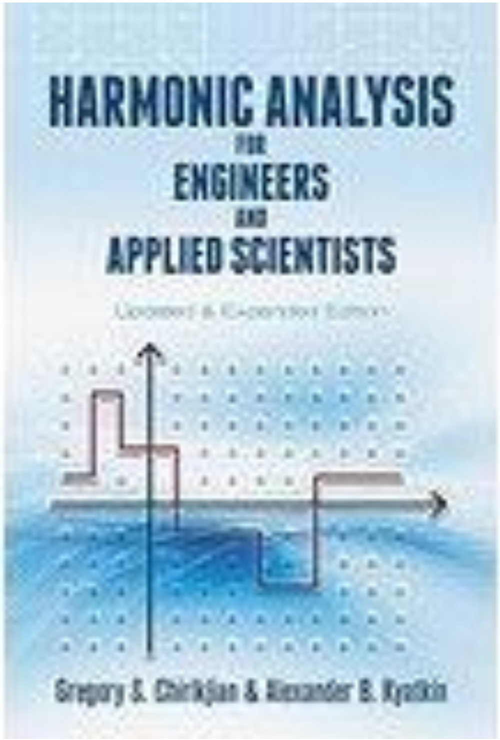

Differential Operators Acting on Functions on SE(N)

$$\tilde{X}_i^R f(H(\vec{q})) = \frac{d}{dt} f(H \circ H_i(t))\Big|_{t=0} = \frac{d}{dt} f(H \circ (I + t\tilde{X}_i))\Big|_{t=0}$$

$$\tilde{X}_i^L f(H(\vec{q})) = \frac{d}{dt} f(H_i(t) \circ H)\Big|_{t=0} = \frac{d}{dt} f((I + t\tilde{X}_i) \circ H)\Big|_{t=0}$$

Differential operators defined for *SE(2)*

$$\tilde{X}_1^R = \frac{\partial}{\partial\phi}$$

$$\tilde{X}_2^R = \cos(\phi-\theta)\frac{\partial}{\partial r} + \frac{\sin(\phi-\theta)}{r}\frac{\partial}{\partial\theta}$$

$$\tilde{X}_3^R = -\sin(\phi-\theta)\frac{\partial}{\partial r} + \frac{\cos(\phi-\theta)}{r}\frac{\partial}{\partial\theta}$$

$$\tilde{X}_1^L = -\frac{\partial}{\partial\phi} - \frac{\partial}{\partial\theta}$$

$$\tilde{X}_2^L = -\cos\theta\frac{\partial}{\partial r} + \frac{\sin\theta}{r}\frac{\partial}{\partial\theta}$$

$$\tilde{X}_3^L = -\sin\theta\frac{\partial}{\partial r} - \frac{\cos\theta}{r}\frac{\partial}{\partial\theta}$$

Differential operators defined for *SE(3)*

$$\tilde{X}_i^R = \begin{cases} X_i^R & \text{for } i = 1,2,3 \\ \left(A^T \nabla_{\vec{a}}\right)_{i-3} & \text{for } i = 4,5,6 \end{cases}$$

$$\tilde{X}_i^L = \begin{cases} X_i^L + \sum_{k=1}^{3} (\vec{a} \times \vec{e}_i) \cdot \vec{e}_k \dfrac{\partial}{\partial a_k} & \text{for } i = 1,2,3 \\ -\dfrac{\partial}{\partial a_{i-3}} & \text{for } i = 4,5,6 \end{cases}$$

Variational Calculus on Lie groups

- Given the functional and constraints

$$J = \int_{t_1}^{t_2} f(g; g^{-1}\dot{g}; t)\, dt, \quad C_k = \int_{t_1}^{t_2} h_k(g)\, dt$$

one can get the Euler-Poincaré equation as:

$$\frac{d}{dt}\left(\frac{\partial f}{\partial \xi_i}\right) + \sum_{j,k=1}^{n} \frac{\partial f}{\partial \xi_k} C_{ij}^{k}\, \xi_j = X_i^R \left(f + \sum_{l=1}^{m} \lambda_l h_l\right),$$

$$X_i^R f(g) = \frac{d}{dt} f(g \circ \exp(tX_i))\Big|_{t=0}$$

where $\left[X_i, X_j\right] = \sum_{k=1}^{6} C_{ij}^{k} X_k$

Probability on Lie Groups

$$\int_G \log^\vee \left(\mu^{-1} \circ g\right) f(g) dg = \mathbf{0}$$

$$\Sigma = \int_G \log^\vee(\mu^{-1} \circ g)[\log^\vee(\mu^{-1} \circ g)]^T f(g) dg$$

$$f(g; \mu, \Sigma) = \frac{1}{(\Sigma)} \exp\left[-\frac{1}{2}\mathbf{y}^T \Sigma^{-1} \mathbf{y}\right]$$

$$\mathbf{y} = \log(\mu^{-1} \circ g)^\vee$$

- Integration of functions on *SO(3)*

$$\int_{SO(3)} f(A)dA = \frac{1}{V}\int_{\vec{q}\in Q} f(A(\vec{q}))\,|\det J(A(\vec{q}))|\,dq_1 dq_2 dq_3$$

e.g. →

$$\int_{SO(3)} f(A)dA = \frac{1}{8\pi^2}\int_0^{2\pi}\int_0^{\pi}\int_0^{2\pi} f(\alpha,\beta,\gamma)\sin\beta d\alpha d\beta d\gamma$$

- Integration of functions on *SE(2)* and *SE(3)*

$$\int_{SE(N)} f(H)dH = \int_{\vec{q}\in Q} f(H(\vec{q}))\,|\det J(H(\vec{q}))|\,dq_1\cdots dq_N$$

e.g. → **SE(2)**

$$dH(\phi, x_1, x_2) = \frac{1}{2\pi} d\phi dx_1 dx_2$$

e.g. → **SE(3)**

$$dH(\alpha,\beta,\gamma,a_1,a_2,a_3) = dA(\alpha,\beta,\gamma)d\vec{a} = \frac{1}{8\pi^2}\sin\beta d\alpha d\beta d\gamma d\phi da_1 da_2 da_3$$

The Adjoint Matrix:

$$Ad_g(X^\vee) = (gXg^{-1})^\vee,$$

If $g = (\mathbf{a}, A)$ then

$$Ad_g = \begin{pmatrix} A & 0 \\ \mathbf{a} \times A & A \end{pmatrix}$$

The Jacobian Matrix:

$$J(\boldsymbol{\chi}) = \left[\left(g^{-1} \frac{\partial g}{\partial \chi_1} \right)^\vee, \cdots, \left(g^{-1} \frac{\partial g}{\partial \chi_6} \right)^\vee \right]$$

The 'Vee' operation:

$$\boldsymbol{\chi} = (\log g)^\vee.$$

The volume element:

$$dg = |J(\boldsymbol{\chi})| d\chi_1 \cdots d\chi_6$$

Convolution:

$$f_{0,2}(g) = (f_{0,1} * f_{1,2})(g) = \int_G f_{0,1}(h) f_{1,2}(h^{-1} \circ g) dh$$

Computing Bounds on the Entropy of the Unfolded Ensemble Using Gaussians on $SE(3)$

We can define the Gaussian in the exponential parameters as

$$f(g(\boldsymbol{\chi})) = \frac{1}{(2\pi)^3|\Sigma|^{\frac{1}{2}}} \exp(-\frac{1}{2}\boldsymbol{\chi}^T\Sigma^{-1}\boldsymbol{\chi}) \tag{1}$$

Given two distributions that are shifted as $f_{i,i+1}(g_{i,i+1}^{-1} \circ g)$, each with 6×6 covariance $\Sigma_{i,i+1}$, then it can be shown that the mean and covariance of the convolution $f_{0,1}(g_{0,1}^{-1} \circ g) * f_{1,2}(g_{1,2}^{-1} \circ g)$ respectively will be of the form $g_{0,2} = g_{0,1} \circ g_{1,2}$ and

$$\Sigma_{0,2} = Ad_{g_{1,2}}^{-1}\Sigma_{0,1}Ad_{g_{1,2}}^{-T} + \Sigma_{1,2}. \tag{2}$$

$$f(g_1, g_2, ..., g_n) = \prod_{i=0}^{n-1} f_{i,i+1}(g_i^{-1} \circ g_{i+1}) \tag{3}$$

where $g_0 = e$, the identity.

The full pose entropy of a phantom chain:

$$S_g = -\int_G \cdots \int_G f(g_1, g_2, ..., g_n) \log f(g_1, g_2, ..., g_n) dg_1 \cdots dg_n. \tag{4}$$

Marginal and conditional entropies can also be computed.

Fourier Analysis of Motion

- Fourier transform of a function of motion, *f(g)*

$$F(f) = \hat{f}(p) = \int_G f(g)U(g^{-1}, p)\,dg$$

- Inverse Fourier transform of a function of motion

$$F^{-1}(\hat{f}) = f(g) = \int trace(\hat{f}(p)U(g, p))\, p^{N-1}\, dp$$

where $g \in SE(N)$, p is a frequency parameter,
$U(g,p)$ is a matrix representation of $SE(N)$, and
dg is a volume element at g.

Convolution and the SE(3) Fourier Transform

$$(f_1 * f_2)(g) = \int_G f_1(h) f_2(h^{-1} \circ g) dh$$

$$F(f_1 * f_2) = F(f_2) F(f_1)$$

G.S. Chirikjian, Stochastic Models, Information Theory, and Lie Groups, Vol. 1, 2, Birkhauser, 2009, 2011.

G.S. Chirikjian, A.B. Kyatkin, Engineering Applications of Noncommutative Harmonic Analysis, CRC Press, 2001.

PART 2: APPLICATIONS TO CONFORMATIONAL ENSEMBLES

Workspace Density

- It describes the density of the reachable frames in the work space.

- It is a probabilistic measurement of accuracy over the workspace.

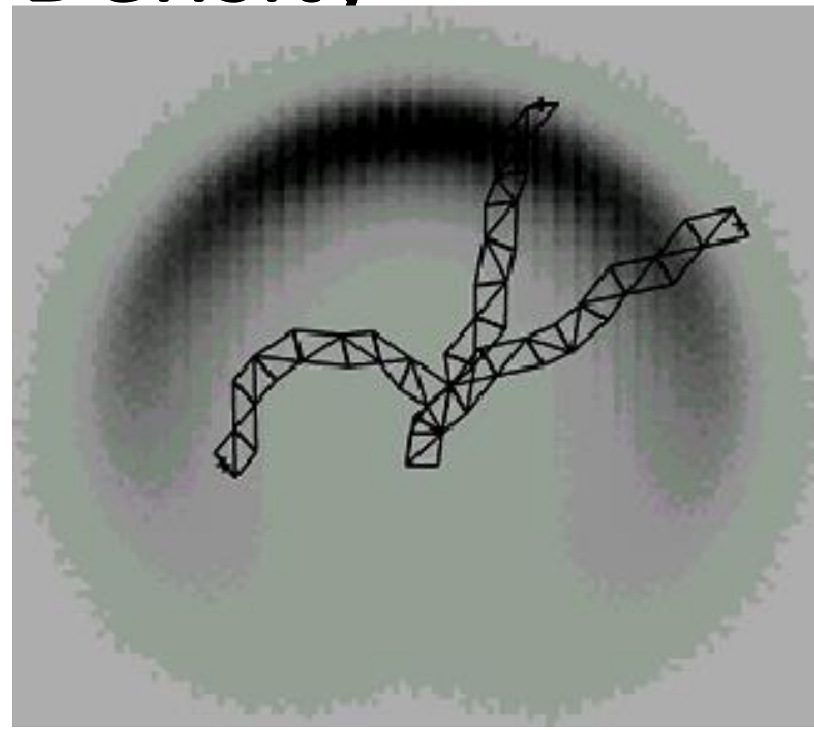

Ebert-Uphoff, I., Chirikjian, G.S., ``Inverse Kinematics of Discretely Actuated Hyper-Redundant Manipulators Using Workspace Densities,'' ICRA'96, pp. 139-145

Long, A.W., Wolfe, K.C., Mashner, M.J., Chirikjian, G.S., ``The Banana Distribution is Gaussian: A Localization Study with Exponential Coordinates,'' RSS, Sydney, NSW, Australia, July 09 - July 13, 2012.

A General Semiflexible Polymer Model

A diffusion equation describing the PDF of relative pose between the frame of reference at arc length s and that at the proximal end of the chain

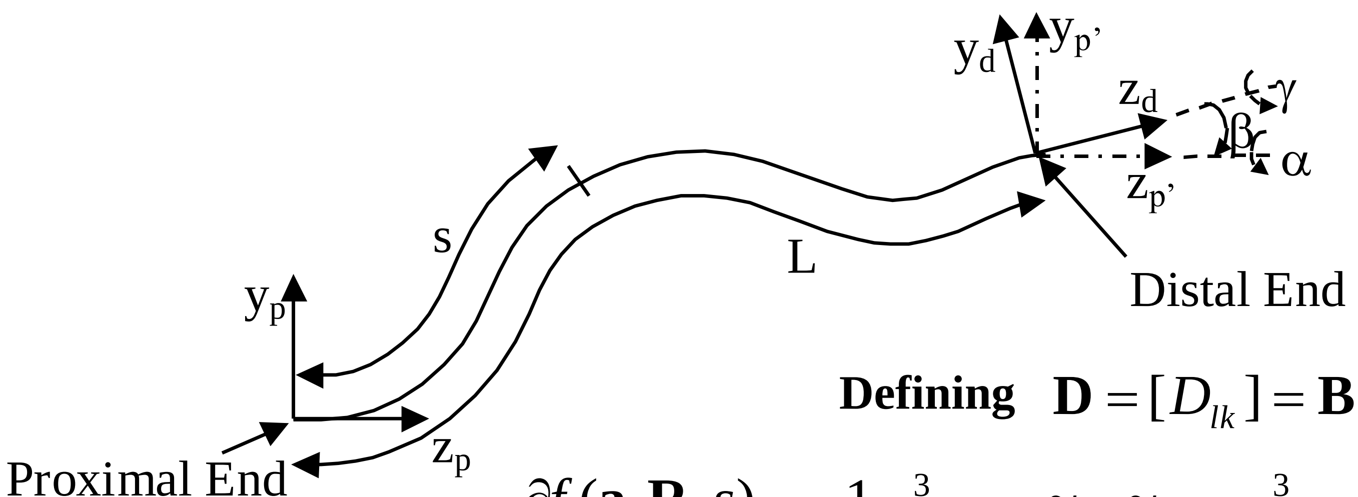

Defining $\mathbf{D} = [D_{lk}] = \mathbf{B}^{-1} \quad \mathbf{d} = [d_l] = -\mathbf{B}^{-1}\mathbf{b}$

$$\frac{\partial f(\mathbf{a}, \mathbf{R}, s)}{\partial s} = \left(\frac{1}{2}\sum_{k,l=1}^{3} D_{lk}\tilde{X}_l^R \tilde{X}_k^R + \sum_{l=1}^{3} d_l \tilde{X}_l^R - \tilde{X}_6^R\right) f(\mathbf{a}, \mathbf{R}, s)$$

Initial condition: f(a,R,0)= δ(a) δ(R)

Operational Properties of SE(n) Fourier Transform

$$F\left(\tilde{X}_i^R f\right) = \int_G \frac{d}{dt}\left(f(g \circ \exp(t\tilde{X}_i))\right)\Big|_{t=0} U(g^{-1}, p)\, d(g)$$

$$\Downarrow^{h = g \circ \exp(t\tilde{X}_i)}$$

$$= \int_G f(h) \frac{d}{dt} U\left(\exp(t\tilde{X}_i) \circ h^{-1}, p\right)\Big|_{t=0} d(h)$$

$$\Downarrow^{U(g_1 \circ g_2, p) = U(g_1, p)U(g_2, p)}$$

$$= \left(\frac{d}{dt} U\left(\exp(t\tilde{X}_i), p\right)\Big|_{t=0}\right)\left(\int_G f(h) U(h^{-1}, p)\, d(h)\right)$$

$$= \eta(\tilde{X}_i, p)\, \hat{f}(p)$$

Explicit Expression of $\eta(\tilde{X}_i, p)$ for *SE(2)*

$$\eta(\tilde{X}_i, p) = \left(\frac{d}{dt} U(\exp(t\tilde{X}_i), p) \right)\Big|_{t-0}$$

$$u_{mn}(g(a,\phi,\theta), p) = i^{n-m} e^{-i[n\theta+(m-n)\phi]} J_{n-m}(pa)$$

$$\eta_{mn}(\tilde{X}_1, p) = -jm\delta_{m,n}$$

$$\eta_{mn}(\tilde{X}_2, p) = \frac{jp}{2}(\delta_{m,n+1} + \delta_{m,n-1})$$

$$\eta_{mn}(\tilde{X}_3, p) = \frac{p}{2}(\delta_{m,n+1} - \delta_{m,n-1})$$

Explicit Expression of $\eta(\tilde{X}_i, p)$ for *SE(3)*

$$\eta(\tilde{X}_i, p) = \left(\frac{d}{dt} U(\exp(t\tilde{X}_i), p) \right)\Big|_{t-0}$$

$$u^{s}_{l',m';l,m}(g, p) = \sum_{k=-l}^{l} [l', m' \mid p, s \mid l, m](\vec{a}) U^{l}_{km}(A)$$

$$\eta_{l',m';l,m}(\tilde{X}_1, p) = \frac{1}{2} c^{l}_{-m} \delta_{l,l'} \delta_{m'+1,m} - \frac{1}{2} c^{l}_{m} \delta_{l,l'} \delta_{m'-1,m}$$

$$\eta_{l',m';l,m}(\tilde{X}_2, p) = \frac{j}{2} c^{l}_{-m} \delta_{l,l'} \delta_{m'+1,m} + \frac{j}{2} c^{l}_{m} \delta_{l,l'} \delta_{m'-1,m}$$

$$\eta_{l',m';l,m}(\tilde{X}_3, p) = -jm \delta_{l,l'} \delta_{m',m}$$

Explicit Expression of $\eta(X_i , p)$ for $SE(3)$

$$\eta_{l',m';l,m}(\tilde{X}_4, p) = -\frac{jp}{2}\gamma^{s}_{l^i,-m'}\delta_{m',m+1}\delta_{l'-1,l} + \frac{jp}{2}\lambda^{s}_{l,m}\delta_{m',m+1}\delta_{l',l} + \frac{jp}{2}\gamma^{s}_{l,m}\delta_{m',m+1}\delta_{l'+1,l}$$
$$+\frac{jp}{2}\gamma^{s}_{l^i,m'}\delta_{m',m-1}\delta_{l'-1,l} + \frac{jp}{2}\lambda^{s}_{l,-m}\delta_{m',m-1}\delta_{l',l} - \frac{jp}{2}\gamma^{s}_{l,-m}\delta_{m',m-1}\delta_{l'+1,l}$$

$$\eta_{l',m';l,m}(\tilde{X}_5, p) = -\frac{p}{2}\gamma^{s}_{l^i,-m'}\delta_{m',m+1}\delta_{l'-1,l} + \frac{p}{2}\lambda^{s}_{l,m}\delta_{m',m+1}\delta_{l',l} + \frac{p}{2}\gamma^{s}_{l,m}\delta_{m',m+1}\delta_{l'+1,l}$$
$$-\frac{p}{2}\gamma^{s}_{l^i,m'}\delta_{m',m-1}\delta_{l'-1,l} - \frac{p}{2}\lambda^{s}_{l,-m}\delta_{m',m-1}\delta_{l',l} + \frac{p}{2}\gamma^{s}_{l,-m}\delta_{m',m-1}\delta_{l'+1,l}$$

$$\eta_{l',m';l,m}(\tilde{X}_6, p) = jp\kappa^{s}_{l^i,m'}\delta_{m',m}\delta_{l'-1,l} + jp\frac{sm}{l(l+1)}\delta_{m',m}\delta_{l',l} + jp\kappa^{s}_{l,m}\delta_{m',m}\delta_{l'+1,l}$$

Solving for the evolving PDF Using the SE(3) FT

$$\frac{\partial f(\mathbf{a},\mathbf{R},s)}{\partial s} = \left(\frac{1}{2}\sum_{k,l=1}^{3} D_{lk}\tilde{X}_l^R \tilde{X}_k^R + \sum_{l=1}^{3} d_l \tilde{X}_l^R - \tilde{X}_6^R\right) f(\mathbf{a},\mathbf{R},s)$$

Applying SE(3) Fourier transform

$$\frac{d\hat{\mathbf{f}}^r}{ds} = \mathbf{B}^r \hat{\mathbf{f}}^r$$

where B is a constant matrix.

Solving ODE

$$\hat{\mathbf{f}}^r(p,s) = e^{s\mathbf{B}^r}$$

Applying inverse transform

$$f(\mathbf{a},\mathbf{R},s) = \frac{1}{2\pi^2}\sum_{r=-\infty}^{\infty}\sum_{l'=|r|}^{\infty}\sum_{l=|r|}^{\infty}\sum_{m'=-l'}^{l'}\sum_{m=-l}^{l}\int_0^{\infty} \hat{f}^r_{l,m;l',m'}(p)U^r_{l',m';l,m}(\mathbf{a},\mathbf{R};p)p^2dp$$

Numerical Examples

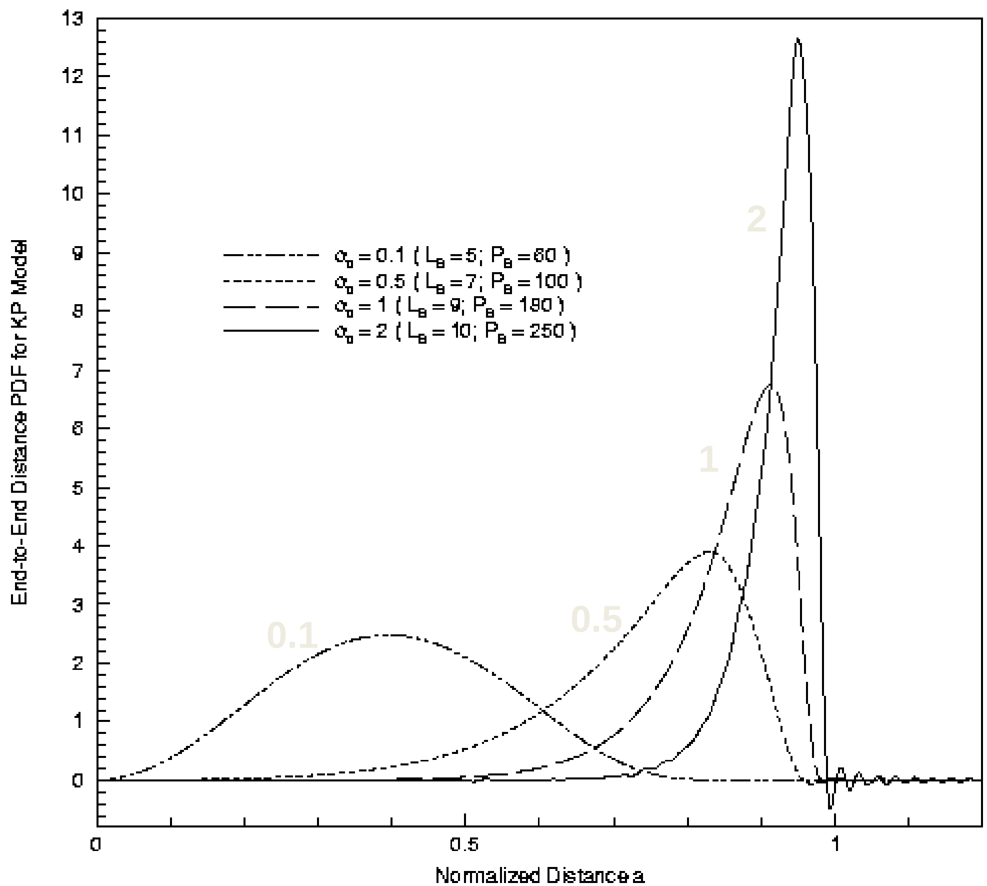

A General Algorithm for Bent or Twisted Macromolecular Chains

The Structure of a Bent Macromolecular Chain

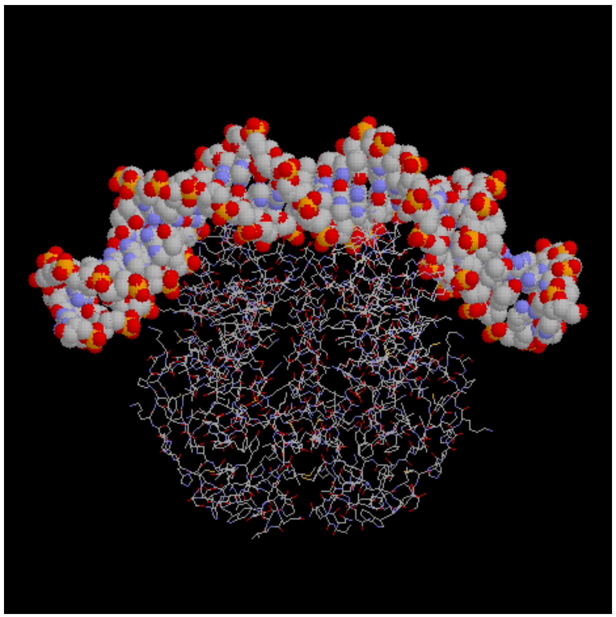

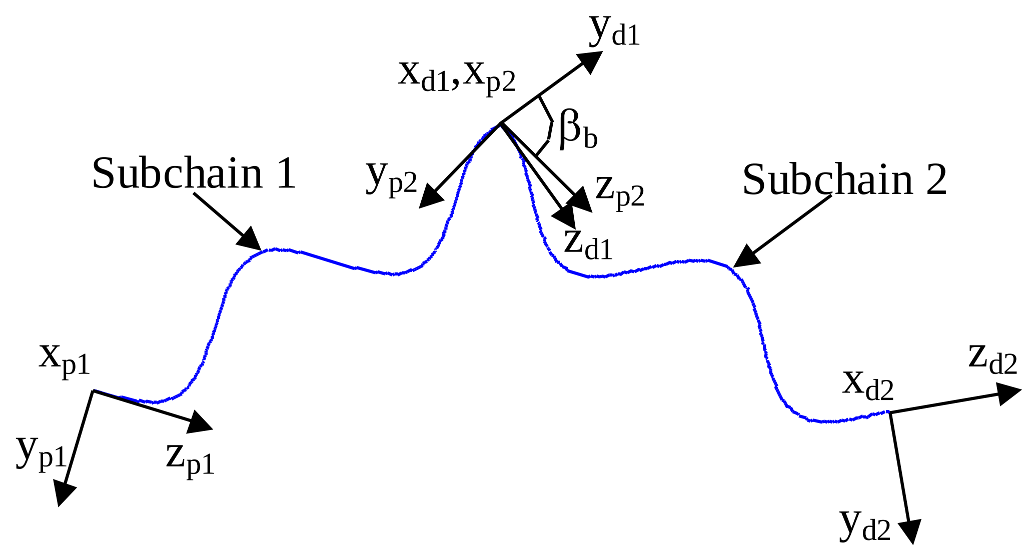

1) **A bent macromolecular chain consists of two intrinsically straight segments.**
2) **A bend or twist is a rotation at the separating point between the two segments with no translation.**

A General Algorithm for Bent or Twisted Macromolecular Chains

The PDF of the End-to-End Pose for a Bent Chain

1) A convolution of 3 PDFs

$$f(\mathbf{a},\mathbf{R}) = (f_1 * f_2 * f_3)(\mathbf{a},\mathbf{R})$$

- $f_1(\mathbf{a},\mathbf{R})$ and $f_3(\mathbf{a},\mathbf{R})$ are obtained by solving the differential equation for nonbent polymer.
- $f_2(\mathbf{a},\mathbf{R}) = \delta(\mathbf{a})\delta(\mathbf{R}_b^{-1}\mathbf{R})$, where $\mathbf{R}_b$ is the rotation made at the bend.

2) The convolution on SE(3)

$$(f_i * f_j)(\mathbf{g}) = \int_{SE(3)} f_i(\mathbf{h}) f_j(\mathbf{h}^{-1} \circ \mathbf{g}) d(\mathbf{h})$$

Examples

1. Variation of f(a) with respect to Bending Angle and Bending Location

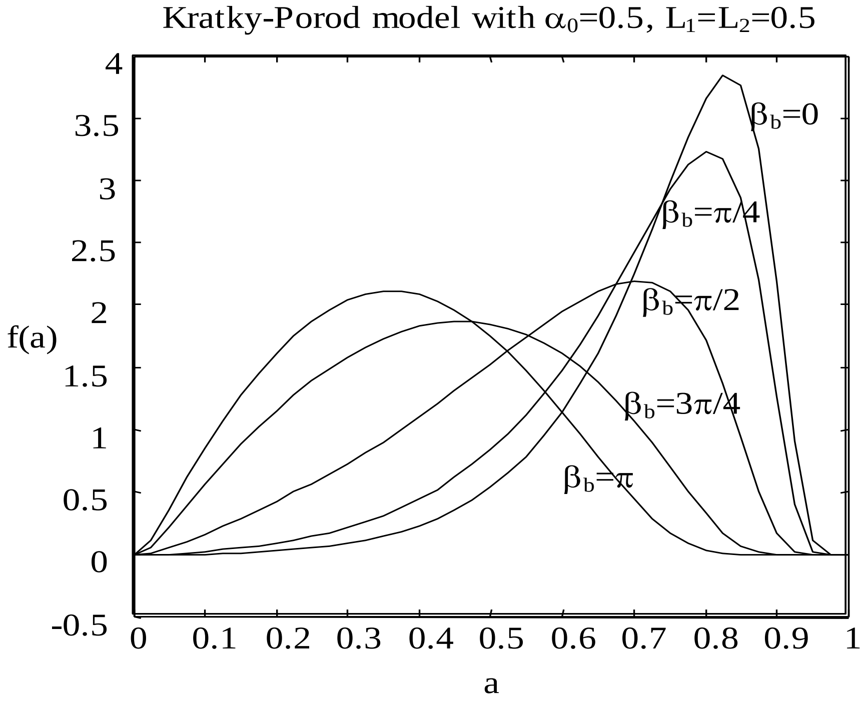

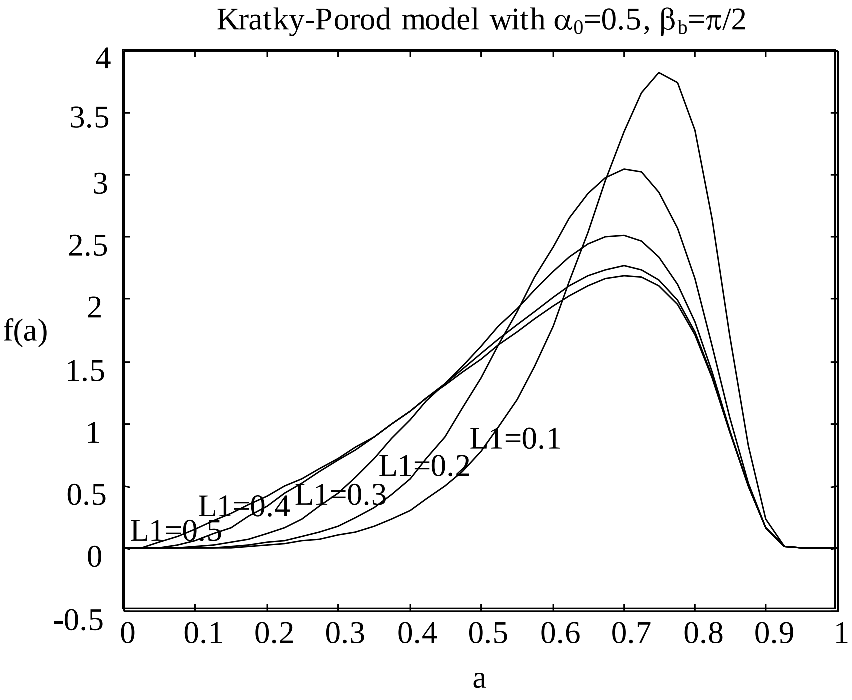

DNA References

1) G. S. Chirikjian, ``Modeling Loop Entropy,'' Methods in Enzymology, 487, 2011

1) Y. Zhou, G. S. Chirikjian, ``Conformational Statistics of Semiflexible Macromolecular Chains with Internal Joints,'' Macromolecules. 39:1950-1960. 2006

1) Zhou, Y., Chirikjian, G.S., "Conformational Statistics of Bent Semi-flexible Polymers", Journal of Chemical Physics, vol.119, no.9, pp.4962-4970, 2003.

2) G. S. Chirikjian, Y. Wang, ``Conformational Statistics of Stiff Macromolecules as Solutions to PDEs on the Rotation and Motion Groups,'' Physical Review E. 62(1):880-892. 2000

PART 4: STOCHASTIC KINEMATICS AND INFORMATION-DRIVEN MOTION

LITERATURE REVIEW

The connection between information theory and sensor fusion in robotics is well known:

Durrant-Whyte, H.F., "Sensor Models and Multisensor Integration," *IJRR*, 7(6):97-113, 1988.

In addition, over the past decade, problems in mobile robotics have received considerable attention. Two classes of problems that both fall under the category of estimation are

Simultaneous Localization and Mapping (SLAM):

Thrun, S., Burgard, W., Fox, D., *Probabilistic Robotics* MIT Press, 2005.

Mourikis, A. Roumeliotis, S., "On the treatment of relative-pose measurements for mobile robot localization," *ICRA'06*

And odor source detection:

Porat, B., Nehorai, A., "Localizing vapor-emitting sources by moving sensors," *IEEE Trans. Signal Processing*, 44 (4):10181021, April 1996.

Russell, R. A. *Odour Detection by Mobile Robots*, World Scientific, Singapore, 1999.

Cortez, R.A., Tanner, H.G., Lumia, R., "Distributed Robotic Radiation Mapping," *ISER'08*

Strategies for odor source localization include "infotaxis"

Vergassola, M., Villermaux, E., Shraiman, B.I., " Infotaxis as a strategy for searching without gradients, " *Nature*, Vol 445, 25 January 2007

Stochastic Models of Mobile Robots

$$g(x, y, \theta) = \begin{pmatrix} \cos\theta & -\sin\theta & x \\ \sin\theta & \cos\theta & y \\ 0 & 0 & 1 \end{pmatrix} \tag{0.1}$$

$$g(x_1, y_1, \theta_1) \circ g(x_2, y_2, \theta_2) =$$

$$g(x_1 + x_2 \cos\theta_1 - y_2 \sin\theta_1, y_1 + x_2 \sin\theta_1 + y_2 \cos\theta_1, \theta_1 + \theta_2).$$

Furthermore, pure translational and rotational motions can be expressed as $e^{tX_1} = g(t, 0, 0)$, $e^{tX_2} = g(0, t, 0)$, and $e^{tX_3} = g(0, 0, t)$ where e^{tX_i} is the matrix exponential and X_1, X_2, X_3 are respectively the matrices

$$\begin{pmatrix} 0 & 0 & 1 \\ 0 & 0 & 0 \\ 0 & 0 & 0 \end{pmatrix}; \begin{pmatrix} 0 & 0 & 0 \\ 0 & 0 & 1 \\ 0 & 0 & 0 \end{pmatrix}; \begin{pmatrix} 0 & -1 & 0 \\ 1 & 0 & 0 \\ 0 & 0 & 0 \end{pmatrix}.$$

Zhou, Y., Chirikjian, G.S., "Probabilistic Models of Dead-Reckoning Error in Nonholonomic Mobile Robots," *ICRA'03*

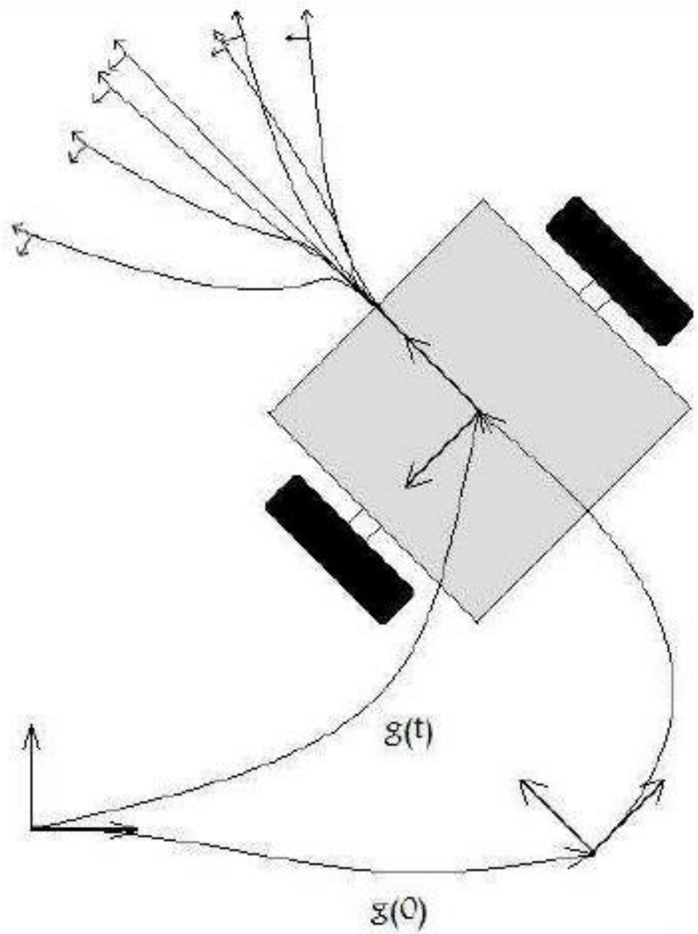

Fig. 0.1. A Kinematic Cart with an Uncertain Future Position and Orientation

$$d\phi_1 = \omega(t)dt + \sqrt{D}dw_1 \tag{0.2}$$
$$d\phi_2 = \omega(t)dt + \sqrt{D}dw_2 \tag{0.3}$$

$$
\begin{pmatrix} dx \\ \\ dy \\ \\ d\theta \end{pmatrix} = \begin{pmatrix} r\omega\cos\theta \\ \\ r\omega\sin\theta \\ \\ 0 \end{pmatrix} dt + \sqrt{D} \begin{pmatrix} \frac{r}{2}\cos\theta & \frac{r}{2}\cos\theta \\ \\ \frac{r}{2}\sin\theta & \frac{r}{2}\sin\theta \\ \\ \frac{r}{L} & -\frac{r}{L} \end{pmatrix} \begin{pmatrix} dw_1 \\ \\ dw_2 \end{pmatrix} \tag{0.4}
$$

Corresponding to an SDE is a Fokker-Planck equation

$$
\frac{\partial f}{\partial t} = -r\omega\cos\theta\frac{\partial f}{\partial x} - r\omega\sin\theta\frac{\partial f}{\partial y} +
$$

$$
\frac{D}{2}\left(\frac{r^2}{2}\cos^2\theta\frac{\partial^2 f}{\partial x^2} + \frac{r^2}{2}\sin 2\theta\frac{\partial^2 f}{\partial x\partial y} + \frac{r^2}{2}\sin^2\theta\frac{\partial^2 f}{\partial y^2} + \frac{2r^2}{L^2}\frac{\partial^2 f}{\partial\theta^2}\right).
$$

There is a very clean coordinate-free way of writing these SDEs and FPEs. Namely,

$$
\left(g^{-1}\frac{dg}{dt}\right)^{\vee} dt = r\omega\mathbf{e}_1 dt + \frac{r\sqrt{D}}{2}\begin{pmatrix} 1 & 1 \\ 0 & 0 \\ 2/L & -2/L \end{pmatrix} d\mathbf{w}
$$

where $\vee$ is the "vee operator" . The coordinate-free version of the Fokker-Planck equation is given below.

Calculus on Euclidean Groups

Analogs of the usual partial derivatives in $\mathbb{R}^n$ can be defined in the Lie-group setting as

$$\tilde{X}_i f = \left[\frac{d}{dt} f\left(g \circ e^{tX_i}\right)\right]\Big|_{t=0}, \; i = 1, 2, 3. \tag{0.5}$$

These are called Lie derivatives. The Fokker-Planck equation above can be written compactly in terms of these Lie derivatives as

$$\frac{\partial f}{\partial t} = -r\omega \tilde{X}_1 f + \frac{r^2 D}{4}(\tilde{X}_1)^2 f + \frac{r^2 D}{L^2}(\tilde{X}_3)^2 f. \tag{0.6}$$

$$\int_G f(g)dg = \int_G f(g_0 \circ g)dg = \int_G f(g \circ g_0)dg = \int_G f(g^{-1})dg.$$

If the robot continues to move for an additional amount of time, t_2, then the distribution will be updated as a convolution over $G = SE(2)$ of the form

$$\boxed{f_{t_1+t_2}(g) = (f_{t_1} * f_{t_2})(g) = \int_G f_{t_1}(h) f_{t_2}(h^{-1} \circ g)dh.} \tag{0.7}$$

It is possible to either solve for this density, or to propagate its moments:

Wang, Y., Chirikjian, G.S., "Nonparametric Second-Order Theory of Error Propagation on the Euclidean Group," *IJRR*, 27(1112): 12581273, 2008.

Park, W., Liu, Y., Zhou, Y., Moses, M., Chirikjian, G.S., "Kinematic State Estimation and Motion Planning for Stochastic Nonholonomic Systems Using the Exponential Map," *Robotica*, 26(4), 419-434. July-August 2008

References

1. Berg, H.C., *E. coli in Motion*, Springer, New York, 2004.
2. Bray, D., *Cell Movements*, Garland Pubishing, Inc., New York and London, 1992.
3. Bullo, F., Lewis, A. D., *Geometric Control of Mechanical Systems*, Springer, 2004.
4. Chirikjian, G.S., Kyatkin, A.B., *Engineering Applications of Noncommutative Harmonic Analysis*, CRC Press, Boca Raton, 2001.
5. Chirikjian, G.S., *Stochastic Models, Information Theory, and Lie Groups*, Birkhäuser, 2009.
6. Kwon, J., Choi, M., Park, F. C., Chu, C., "Particle filtering on the Euclidean group: framework and applications, " *Robotica*, Vol. 25, pp. 725737, 2007.
7. Park, W., Kim, J.S., Zhou, Y., Cowan, N.J., Okamura, A.M., Chirikjian, G.S., "Diffusion-based motion planning for a nonholonomic flexible needle model," *ICRA'05*
8. Patlak, C.S., "A mathematical contribution to the study of orientation of organisms," *Bulletin of Mathematical Biophysics*, Vol. 15, 1953. pp. 431-476.

Flexible Needles with Bevel tip

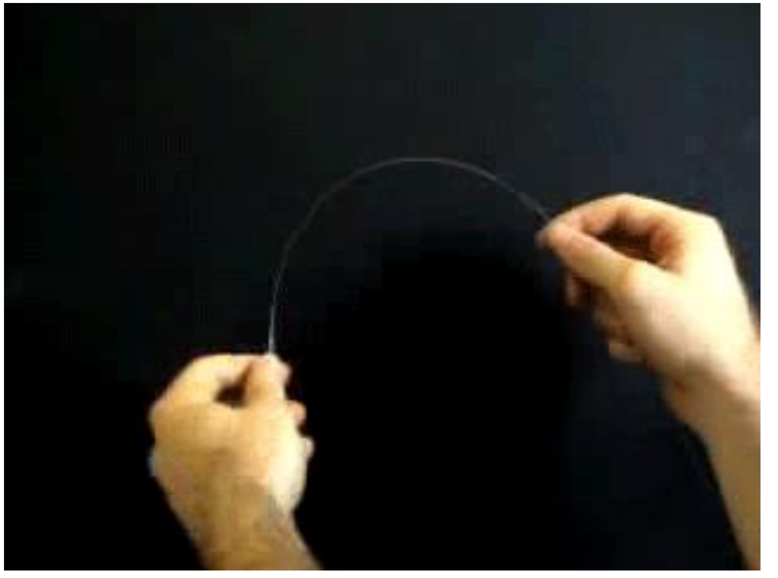

http://research.vuse.vanderbilt.edu/MEDLab/research_files/needlesteer.htm

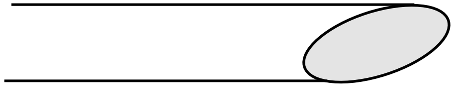

Needle with a bevel tip

Needle Model

- **Deterministic nonholonomic model**

$$\xi = \begin{bmatrix} \omega_x \\ \omega_y \\ \omega_z \\ v_x \\ v_y \\ v_z \end{bmatrix} = \begin{bmatrix} \kappa v \\ 0 \\ \omega \\ 0 \\ 0 \\ v \end{bmatrix}$$

v **: insertion speed** ω **: twisting angular velocity**

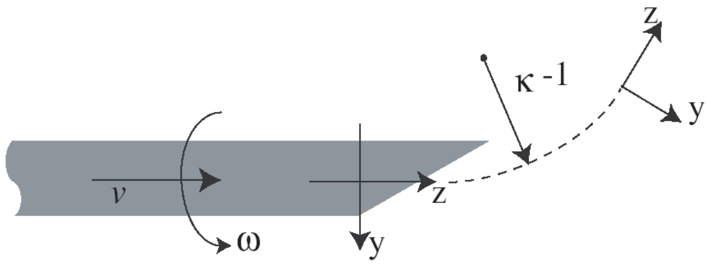

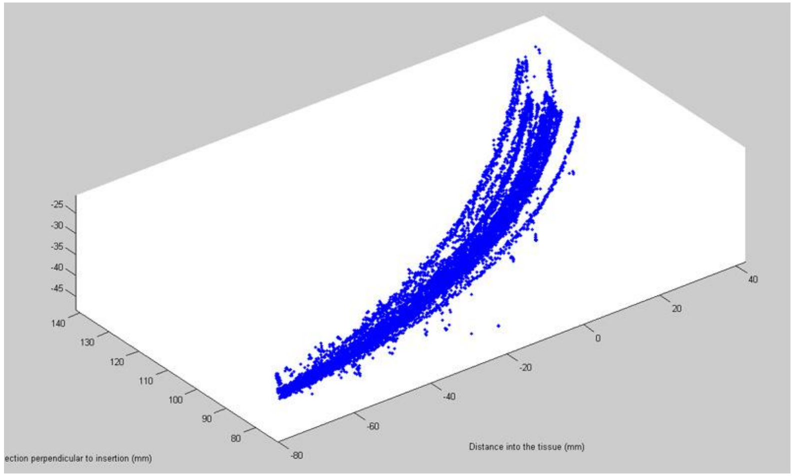

Experiments by Dr. Kyle Reed

Stochastic needle model

$$\omega(t) = \lambda_1 w_1(t)$$

$$v(t) = 1 + \lambda_2 w_2(t)$$

$w_i(t)$: Unit Gaussian white noise

λ_i : Strength of noise

$$(g^{-1}\dot{g})^{\vee} dt = \begin{bmatrix}\kappa & 0 & 0 & 0 & 0 & 1\end{bmatrix}^{\mathrm{T}} dt + \begin{bmatrix} 0 & 0 & \lambda_1 & 0 & 0 & 0 \\ \kappa\lambda_2 & 0 & 0 & 0 & 0 & \lambda_2 \end{bmatrix}^T \begin{bmatrix} d\mathrm{W}_1 \\ d\mathrm{W}_2 \end{bmatrix}$$

g : SE(3) frame for needle tip pose

$\mathrm{W}_i(t)$ **:** Wiener process

Park, W., Kim, J.S., Zhou, Y., Cowan, N.J., Okamura, A.M., Chirikjian, G.S., ``Diffusion-based motion planning for a nonholonomic flexible needle model,'' ICRA'05, Barcelona, Spain

Park, W., Reed, K. B., Okamura, A. M., Chirikjian, G. S., ``Estimation of model parameters for steerable needles,'' ICRA, Anchorage, Alaska, 2010.

References

1) Chirikjian, G.S. "A binary paradigm for robotic manipulators.“ ICRA 1994. pp. 3063-3069.

2) Ebert-Uphoff, I., Chirikjian, G.S., ``Inverse Kinematics of Discretely Actuated Hyper-Redundant Manipulators Using Workspace Densities,'‘ ICRA 1996, 139-145.

3) Chirikjian, G.S., Burdick, J.W., ``An Obstacle Avoidance Algorithm for Hyper-Redundant Manipulators,'' ICRA 1990, 625-631.

4) Park, W., Wang, Y., Chirikjian, G.S., ``The path-of-probability algorithm for steering and feedback control of flexible needles,'‘ International Journal of Robotics Research, Vol. 29, No. 7, 813-830 (2010)

Other References

Alterovitz, R., Lim, A., Goldberg, K., Chirikjian, G.S., Okamura, A.M., ``Steering flexible needles under Markov motion uncertainty,'' IROS, pp. 120-125, August 2005.

R. J. Webster III, J. S. Kim, N. J. Cowan, G. S. Chirikjian and A. M. Okamura, "Nonholonomic Modeling of Needle Steering," International Journal of Robotics Research, Vol. 25, No. 5-6, pp. 509-525, May-June 2006.

Park, W., Wang, Y., Chirikjian, G.S., ``The path-of-probability algorithm for steering and feedback control of flexible needles,'‘ IJRR, Vol. 29, No. 7, 813-830 (2010)

Entropy and Relative Entropy on Euclidean Groups

Equipped with a method to integrate, all of the classical definitions of continuous information theory can be generalized to the group setting. Namely, the Shannon entropy and Kullback-Leibler divergence become

$$\boxed{S(f) = -\int_G f(g)\log f(g)dg}$$

and

$$\boxed{D_{KL}(f \,\|\, \phi) = \int_G f(g)\log\left(\frac{f(g)}{\phi(g)}\right) dg}$$

where $f(g)$ and $\phi(g)$ are probability density functions (i.e., they are non-negative functions that integrate to unity). Furthermore, many information inequalities formulated in Euclidean space also hold in the context of Lie groups, as exemplified by the following.

Theorem 1: The entropy of convolved pdfs increase, and the data processing inequality holds:

$$S(f_1 * f_2) \geq \max\{S(f_1), S(f_2)\}$$

and

$$D_{KL}(f_1 \,\|\, f_2) \geq \max\left\{D_{KL}(f_1 * \phi \,\|\, f_2 * \phi), D_{KL}(\phi * f_1 \,\|\, \phi * f_2)\right\}.$$

Proof: Follows from the convexity of the functions $-\log x$ and $x \log x$, and Jensen's inequality, and the joint convexity of $D_{KL}(\cdot \,\|\, \cdot)$.

Gaussian Approximation of Non-linear Measurement Models on Lie Groups

Greg Chirikjian and Marin Kobilarov
Johns Hopkins University

December 17, 2014
CDC, Los Angeles

GC's presentation is supported by the NSF IRD Program

Motivation

- Filering on manifolds vs coordinates
  - avoid singularities/chart switching
  - employ natural distance metrics
  - capture nonlinearities
- Rich literature for filtering on manifolds
  - Euclidean group filtering: Lo, Tsiotras, Junkins, Markley, Hamel, Mahony, Chirikjian, etc...
  - General Lie group filtering: Absil, Mahony, Bonnabel et al, Manton, Bourmaud et al, Leok et al, Chirikjian, etc..
- Our focus
  - show advantages of Lie group representation for range-bearing models
  - second-order accurate measurement update using moment matching
  - can be used for increasing filtering accuracy on any Lie group

SDE for the Kinematic Cart

(Zhou and Chirikjian, ICRA 2003)

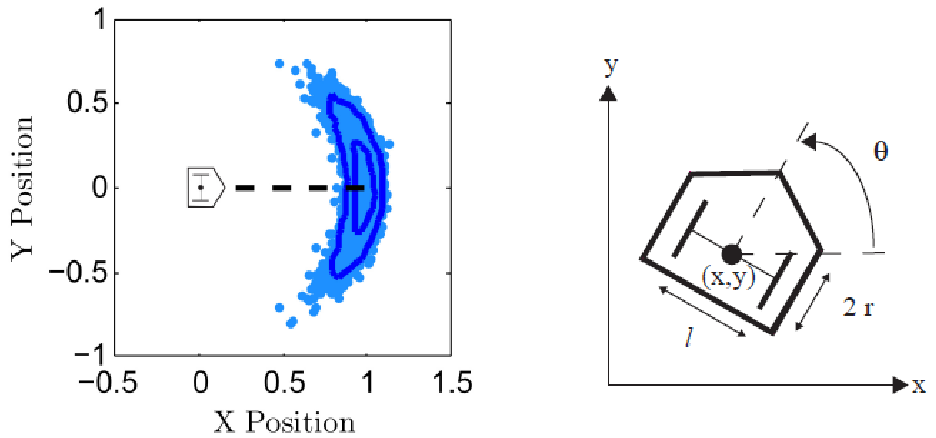

(a) (b)

$$\begin{pmatrix} dx \\ dy \\ d\theta \end{pmatrix} = \begin{pmatrix} \frac{r}{2}(\omega_1 + \omega_2)\cos\theta \\ \frac{r}{2}(\omega_1 + \omega_2)\sin\theta \\ \frac{r}{\ell}(\omega_1 - \omega_2) \end{pmatrix} dt + \sqrt{D} \begin{pmatrix} \frac{r}{2}\cos\theta & \frac{r}{2}\cos\theta \\ \frac{r}{2}\sin\theta & \frac{r}{2}\sin\theta \\ \frac{r}{\ell} & -\frac{r}{\ell} \end{pmatrix} \begin{pmatrix} dw_1 \\ dw_2 \end{pmatrix}$$

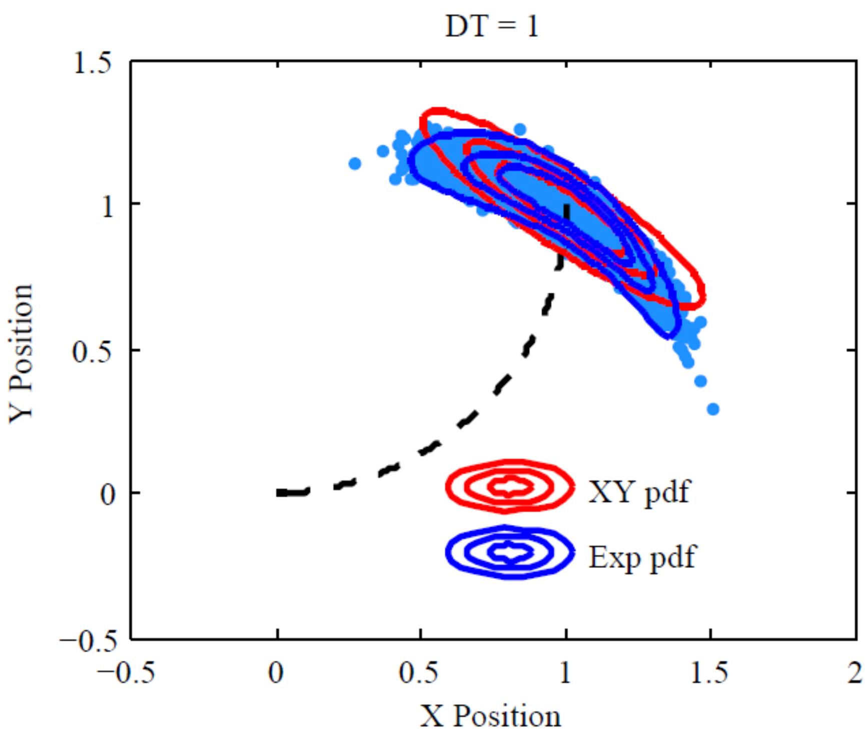

Long et al, ``The Banana Distribution is Gaussian'' RSS 2012

$$\int_G \log^\vee\left(\mu^{-1} \circ g\right) f(g) dg = \mathbf{0} \qquad \Sigma = \int_G \log^\vee(\mu^{-1} \circ g)[\log^\vee(\mu^{-1} \circ g)]^T f(g) dg$$

$$f(g; \mu, \Sigma) = \frac{1}{c(\Sigma)} \exp\left[-\frac{1}{2}\mathbf{y}^T \Sigma^{-1} \mathbf{y}\right] \qquad \mathbf{y} = \log(\mu^{-1} \circ g)^\vee$$

Exponential Coordinates for SE(2)

$$
\begin{aligned}
g(v_1, v_2, \alpha) &= \exp(X) \\
&= \begin{pmatrix} \cos\alpha & -\sin\alpha & t_1 \\ \sin\alpha & \cos\alpha & t_2 \\ 0 & 0 & 1 \end{pmatrix}
\end{aligned}
$$

$$
\begin{aligned}
t_1 &= [v_2(-1 + \cos\alpha) + v_1 \sin\alpha]/\alpha \\
t_2 &= [v_1(1 - \cos\alpha) + v_2 \sin\alpha]/\alpha.
\end{aligned}
$$

Introduction

Consider a simple example: robot localization

- one beacon: large uncertainty (not fully observable)

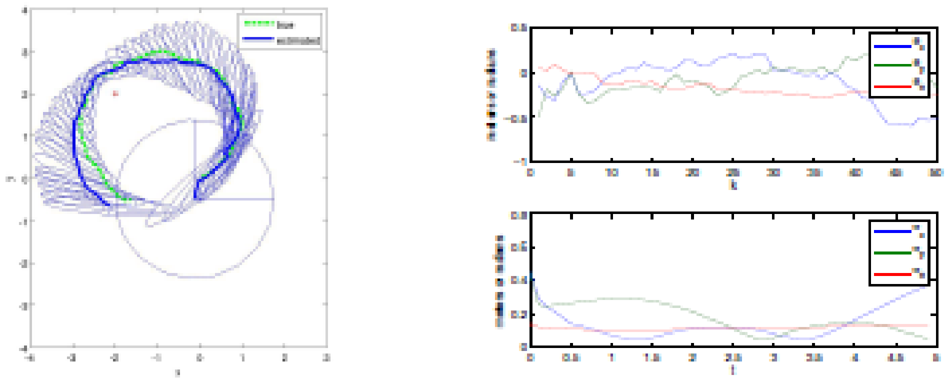

- two beacons: low uncertainty (fully observable)

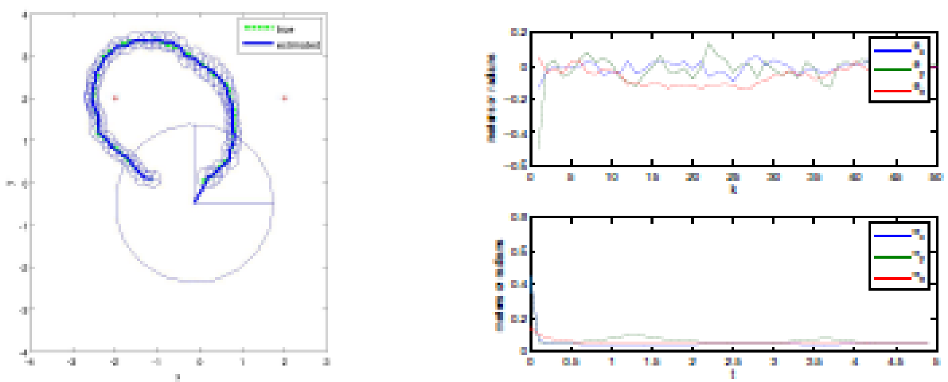

Measurement Models

Consider an autonomous vehicle in workspace $\mathcal{W} \subset \mathbb{R}^2$ or $\mathcal{W} \subset \mathbb{R}^3$

- pose $g \in G$ where $G = SE(2)$ or $G = SE(3)$

$$g = \begin{bmatrix} R & x \\ 0 & 1 \end{bmatrix},$$

  with rotation matrix R and position $x \in \mathcal{W}$
- random measurement z taking values in $\mathbb{R}^m$ defined by

$$z = h(g) + H(g)n.$$

  where n is a noise vector and $H(g)$ is a coupling matrix
- pdf of n is $q_n : \mathbb{R}^m \to \mathbb{R}_{\geq 0}$,
- pdf for given $g \in G$ is then defined by

$$\rho(z \,|\, g) = \frac{1}{|H(g)|} q_n \left([H(g)]^{-1}[z - h(g)] \right). \tag{1}$$

Measurement Models (cont)

- For simplicity assume $H(g) \equiv H$ and let $n \sim \mathcal{N}(0, N)$, $N = HH^T$:

$$\rho(z|g) = \frac{1}{(2\pi)^{\frac{m}{2}}|N|^{\frac{1}{2}}} \exp\left(-\frac{1}{2}[z - h(g)]^T N^{-1} [z - h(g)]\right). \tag{2}$$

- Generate a pdf for g according to

$$\rho_n(g) \equiv \rho(g|z) \doteq \frac{\rho(z\,|\,g)}{\int_G \rho(z\,|\,g) dg},$$

or if a nominal $\rho_0(g)$ is known (i.e. a prior on G) then we have

$$\rho(g|z) \doteq \frac{\rho(z\,|\,g)\rho_0(g)}{\int_G \rho(z\,|\,g)\rho_0(g) dg}. \tag{3}$$

Example Models

- Typically the sensor measures fixed environmental features $\ell \in \mathcal{W}$

$$h(g) = \bar{h}(g^{-1} \cdot \ell)$$

  where $g^{-1} \cdot \ell$ is a left action of G on $\mathcal{W}$, i.e. $g^{-1} \cdot \ell = R^T(\ell - x)$
- Range-bearing in 2D (e.g. 2d LiDAR sensor)

$$\bar{h}_{RB}(y) = \begin{pmatrix} \|y\| \\ \operatorname{arctan2}(y_2, y_1) \end{pmatrix},$$

  for a given $y \in \mathbb{R}^2$
- Monocular camera (MC):

$$\bar{h}_{MC}(y) = \frac{y}{\|y\|},$$

  for a given $y \in \mathbb{R}^3$, using a spherical projection model

Optimal estimation of Gaussians on Lie Groups

- A concentrated Gaussian on an d-dimensional Lie group can be defined as

$$f(g;\mu,\Sigma) \doteq \frac{1}{(2\pi)^{d/2}|\Sigma|^{\frac{1}{2}}} \exp\left(-\frac{1}{2}\left\|\log(\mu^{-1}g)^{\vee}]\right\|^2_{\Sigma^{-1}}\right), \tag{4}$$

  where $\log : G \to \mathfrak{g}$ is the Lie group logarithm, and $\mathfrak{g}$ denotes the Lie algebra
- Goal: find parametric $f(g;\mu,\Sigma)$ that is closest to $\rho(g|z)$
- In the Kullback-Liebler (KL) sense, this is the solution to the optimization problem

$$\min_{\mu,\Sigma} \mathrm{KL}\left(\rho(g|z) \parallel f(g;\mu,\Sigma)\right), \tag{5}$$

  where the KL distance between two given densities $p(g)$ and $q(g)$ is defined by

$$\mathrm{KL}(p \parallel q) = \int_G p(g) \log \frac{p(g)}{q(g)} dg.$$

Optimal estimation of Gaussians on Lie Groups (cont)

- The optimization problem (5) is then equivalent to

$$\min_{\mu,\Sigma} \int_G -\rho(g|z) \log f(g;\mu,\Sigma) dg$$

- solved using the parameterization of:
  - the mean according to $\mu = \mu_0 \exp(\epsilon)$ for some $\epsilon \in \mathfrak{g}$
  - the covariance Σ using its Cholesky factor A such that $\Sigma^{-1} = A^T A$
- the problem is then:

$$\min_{\epsilon,A} \left\{ -\sum_{i=1}^{d} \log A_{ii} + \frac{1}{2} \int_G \rho(g|z) \left\| \log(\exp(-\epsilon)\mu_0^{-1} g)^\vee \right\|^2_{A^T A} dg \right\}.$$

- an can be solved using sampling:

$$\min_{\epsilon,A} \left\{ -\sum_{i=1}^{d} \log A_{ii} + \frac{1}{2} \sum_{i=1}^{N_s} \frac{\rho(z|g_i)}{\sum_{i=1}^{N_s} \rho(z|g_i)} \left\| \log(\exp(-\epsilon)\mu_0^{-1} g_i)^\vee \right\|^2_{A^T A} \right\},$$

where $g_i \in G$ are N_s i.i.d. samples from $\rho_0(g)$

Distribution update using range-bearing measurements

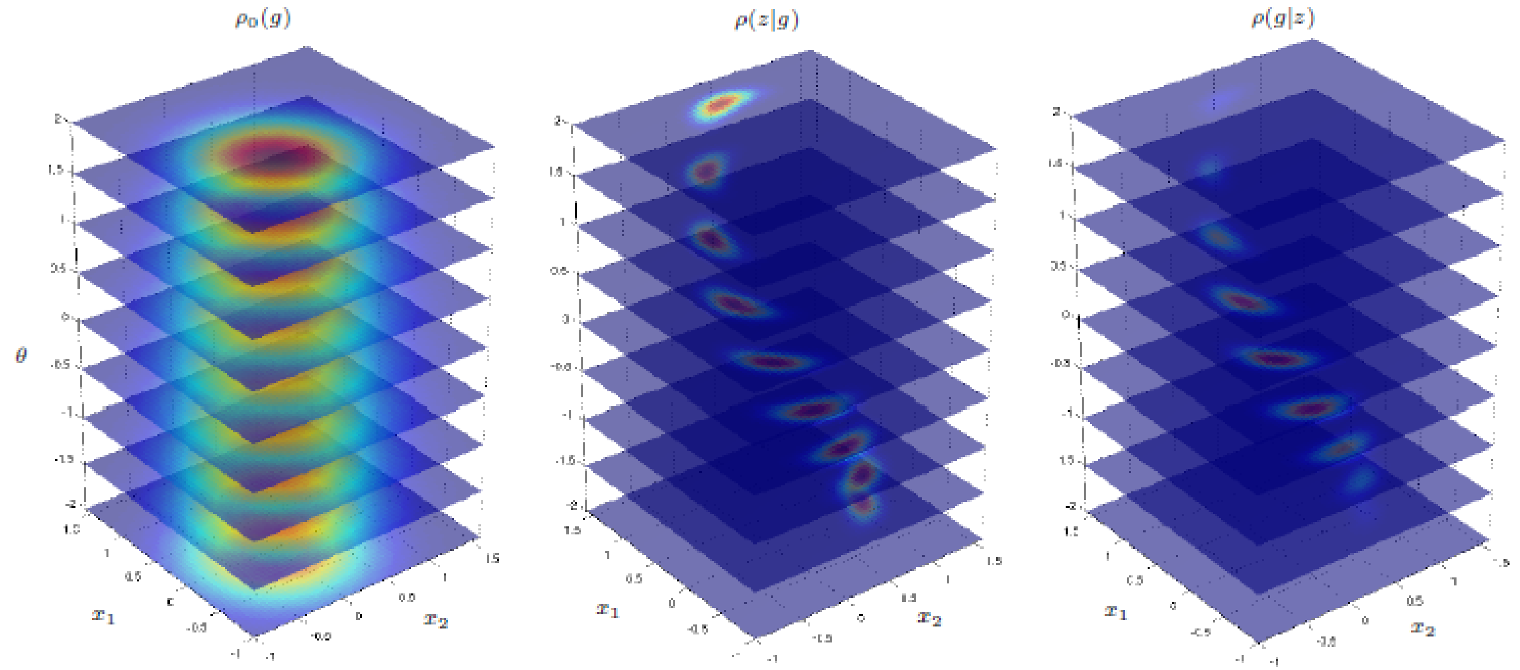

a) prior $\rho_0(g)$

b) meas. model $\rho(z|g)$

c) combined density $\rho(g|z)$

- Note: all densities above displayed in $q = (x_1, x_2, \theta)$ for clarity
- density $\rho(g|z)$ is the full (non-parametric) nonlinear (and non-Gaussian in pose space) density that we aim to approximate.

Coordinate vs Lie-group Gaussian approximations

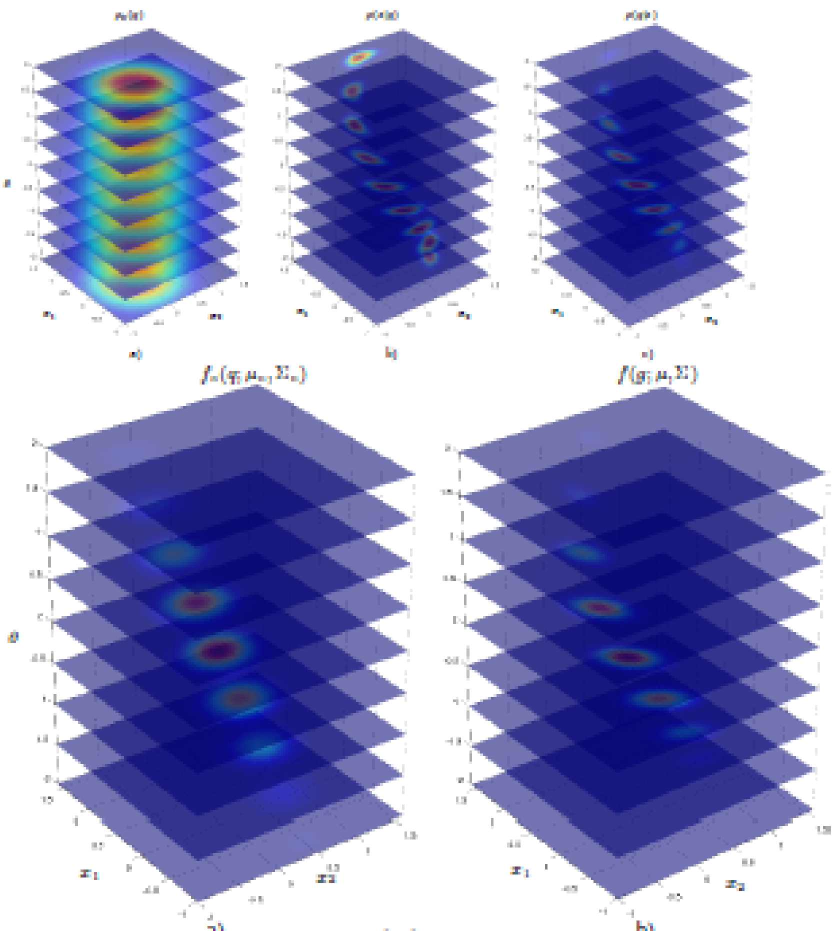

coordinate Gaussian $f_c(q)$ Lie-group Gaussian $f(g)$

Euclidean Gaussian
$\mathrm{KL}(\rho(g\|z) \,\|\, f_c(q)) \approx 1.42$
$\|q_0 - \hat{q}\| \approx .025$

Lie group Gaussian
$\mathrm{KL}(\rho(g\|z) \,\|\, f(g)) \approx 0.67$
$\|q_0 - \hat{q}\| \approx .013$

Second-order expansion of nonlinear model

- A second-order Taylor series for $h(g)$ can be written as

$$e^{\eta} = \mu^{-1} \circ g \qquad h(g) \approx h(\mu) + \sum_{i=1}^{d} \eta_i (\partial_i h)(\mu) + \frac{1}{2} \sum_{i,j=1}^{d} \eta_i \eta_j (\partial_i \partial_j h)(\mu) \tag{6}$$

where here ∂_i is shorthand defined as

$$(\partial_i h)(\mu) = \frac{d}{ds} h(\mu\, e^{sE_i}) \Big|_{s=0} .$$

- the exponent can be written as

$$c(\eta) \doteq -\frac{1}{2}(a + 2b^T \eta + \eta^T K \eta) \tag{7}$$

where

$$a = [h(\mu) - z]^T N^{-1} [h(\mu) - z]$$
$$b_i = [h(\mu) - z]^T N^{-1} (\partial_i h)(\mu)$$
$$K_{ij} = [(\partial_i h)(\mu)]^T N^{-1} (\partial_j h)(\mu) + [h(\mu) - z]^T N^{-1} (\partial_i \partial_j h)(\mu)$$

Measurement PDFs Described as G-Gaussians

- What G-Gaussian best approximates

$$\rho_n(\mu \circ e^{\eta}) \approx \frac{|K|^{\frac{1}{2}}}{(2\pi)^{d/2}} e^{-\frac{c(\eta)}{2}} \quad ?,$$

  i.e. we seek

$$f(\mu \circ e^{\eta}; \mu_n, \Sigma_n) = f(e^{\eta}; \mu^{-1} \circ \mu_n, \Sigma_n)$$

  to match to $\rho_n(\mu \circ e^{\eta})$ when $\mu^{-1} \circ \mu_n$ is close to the identity and the eigenvalues of Σ_n are small.

- Approach: expand density using local parametrization

$$e^{\epsilon} = \mu^{-1} \circ \mu_n \quad \text{and} \quad e^{\eta} = \mu^{-1} \circ g.$$

  and use BCH formula

$$\begin{aligned} \log^{\vee}(e^{-\epsilon} \circ e^{\eta}) \approx & -\epsilon^{\vee} + \eta^{\vee} - \frac{1}{2} ad(\epsilon)\eta^{\vee} \\ & + \frac{1}{12}[ad(\epsilon)ad(\epsilon)\eta^{\vee} - ad(\eta)ad(\eta)\epsilon^{\vee}]. \end{aligned} \tag{8}$$

  to obtain first and second-order terms

Matching 2nd Order Taylor Series and 2nd Order BCH Expansions

Both are of the form

$$c(\eta) \doteq -\frac{1}{2}(a + 2b^T\eta + \eta^T K\eta)$$

We match a, b, K for each.

Moment-matching conditions

As a result we need to compute the uknown ϵ and Σ_n to satisfy:

$$(\epsilon^\vee)^T \Sigma_n^{-1} \epsilon^\vee = a \tag{9}$$

$$-(\epsilon^\vee)^T \Sigma_n^{-1} \left[\mathbb{I}_d - \frac{1}{2} ad(\epsilon) + \frac{1}{12} ad(\epsilon) ad(\epsilon) \right] = b^T \tag{10}$$

and

$$\begin{aligned} &\left[\mathbb{I}_d - \frac{1}{2} ad(\epsilon) + \frac{1}{12} ad(\epsilon) ad(\epsilon) \right]^T \Sigma_n^{-1} \\ &\cdot \left[\mathbb{I}_d - \frac{1}{2} ad(\epsilon) + \frac{1}{12} ad(\epsilon) ad(\epsilon) \right] + M = K \end{aligned} \tag{11}$$

where

$$M_{ij} = \frac{1}{12} (\epsilon^\vee)^T \left[ad_{E_j}^T ad_{E_i}^T \Sigma_n^{-1} + \Sigma_n^{-1} ad_{E_i} ad_{E_j} \right] \epsilon^\vee . \tag{12}$$

Solution using a *perturbation* approach

- simplest zeroth-order approximation from (10) and (11) results in $\Sigma_n \approx K^{-1}$ and $\epsilon \approx -K^{-1}b$
- Note that is the standard EKF on Lie groups (i.e. using first-order linearization)
- Such approximation is valid under the assumption that both $\|\Sigma_n\|$ and $\|\epsilon\|$ are small relative to 1
- We next consider high-order versions:

Case 1: $\nu = O(\|\Sigma_n\|) = O(\|\epsilon\|)$.

Following a standard perturbation approach one can show the a first-order approximation requires the solution of the equations

$$\Sigma_n^{-1} = (\mathbb{I} - A_1^T + B^T)K(\mathbb{I} - A_1 + B), \tag{13}$$

$$\epsilon^\vee = -(\mathbb{I} + A_1 + C)K^{-1}b \tag{14}$$

where

$$A_1 = \frac{1}{2} ad\left(\widehat{K^{-1}b}\right), \quad A_2 = \frac{1}{12} ad\left(\widehat{K^{-1}b}\right) ad\left(\widehat{K^{-1}b}\right)$$

The matrix B is computed from the linear relationship

$$B^T K + KB = [-A_2 + A_1^2]^T K[-A_2 + A_1^2] - M. \tag{15}$$

after which the matrix C is computed to satisfy the equation

$$B^T - K(A_1^2 - B - C)K^{-1} = [-A_2 + A_1^2]^T. \tag{16}$$

The procedure can be performed once or iterated multiple times until the variables Σ_n, ϵ converge. These terms are initialized using the zeroth order solution.

Case 2: $\|\Sigma_n\| = O(\nu)$ and $\|\epsilon\| = O(\nu^2)$.

We again start with (13) and (14) and the same lowest order approximations $\Sigma_n \approx K^{-1}$ and $b_n \approx -K^{-1}b$. But in this scenario, we take $A_2 = \mathbb{O}$ since ϵ is already $O(\nu)$-times smaller than Σ_n. Therefore, in the first order matching does not appear and we solve the following linear equation (which is a modified version of (16) given the above constraints)

$$B^T - KBK^{-1} = -A_1^T$$

for B, which is the only second-order correction, along with

$$\Sigma_n = K^{-1} - BK^{-1} - K^{-1}B^T, \quad \epsilon^\vee = -K^{-1}b.$$

Case 3: $||\Sigma_n|| = O(\nu^2)$ and $||\epsilon|| = O(\nu)$.

In this scenario $B = \mathbb{O}$ because corrections at this level are not required for Σ_n. We then have

$$\Sigma_n = K^{-1} + A_1 K^{-1} + K^{-1} A_1^T, \quad \epsilon^\vee = -(\mathbb{I} + A_1 + C)K^{-1} b.$$

Conclusions

- Gaussians on Lie groups better capture nonlinearities
- Improve measurement update accuracy, can be significant for large covariances
- Higher-order methods are applicable at extra computational cost
- Need to study the trade-off between accuracy and CPU time
- Future/ongoing work: vehicle localization/mapping/tracking

If you like this …

Have a look at my book:

``Stochastic Models, Information Theory, and Lie Groups’’

International Conference on Robotics and Automation
June 2014

An Information-Theoretic Approach to the Correspondence-Free AX=XB Sensor Calibration Problem

M. Kendal Ackerman[1], Alexis Cheng[2]
and Gregory Chirikjian[1]
[1]Dept. Mech. Engineering,
[2]Dept. Computer Science
Johns Hopkins University, Baltimore, MD, USA

RPK
Robot and Protein Kinematics Laboratory

Outline

- The AX=XB Problem
- Notation and Probability Theory Review
- Solution Constraints
- An information Theoretic Approach
- Results and Conclusions

AX = XB is one of the most common mathematical formulations used in robot-sensor calibration problems. It can be found in a variety of applications including:

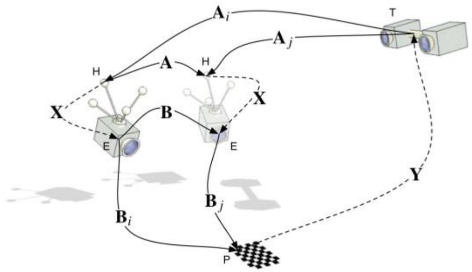

Courtesy: CAMP at TUM

Camera calibration [1]

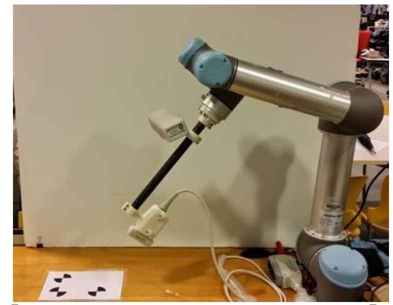

Robot eye-to-hand calibration [1]

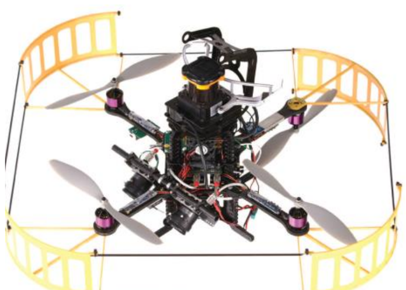

Courtesy: Darius Burschka

Aerial vehicle sensor calibration [2]

Image guided therapy (IGT) sensor calibration [3]

[1] Tsai, R., Lenz, R. (1989)
[2] Mair, E., Fleps, M., Suppa, M., Burschka, D. (2011)
[3] Boctor, E.M. (2006)

AX=XB

$A^{ij} = A_i A_j^{-1}$

$B^{ij} = B_i^{-1} B_j$

$A^{ij} X = X B^{ij}$

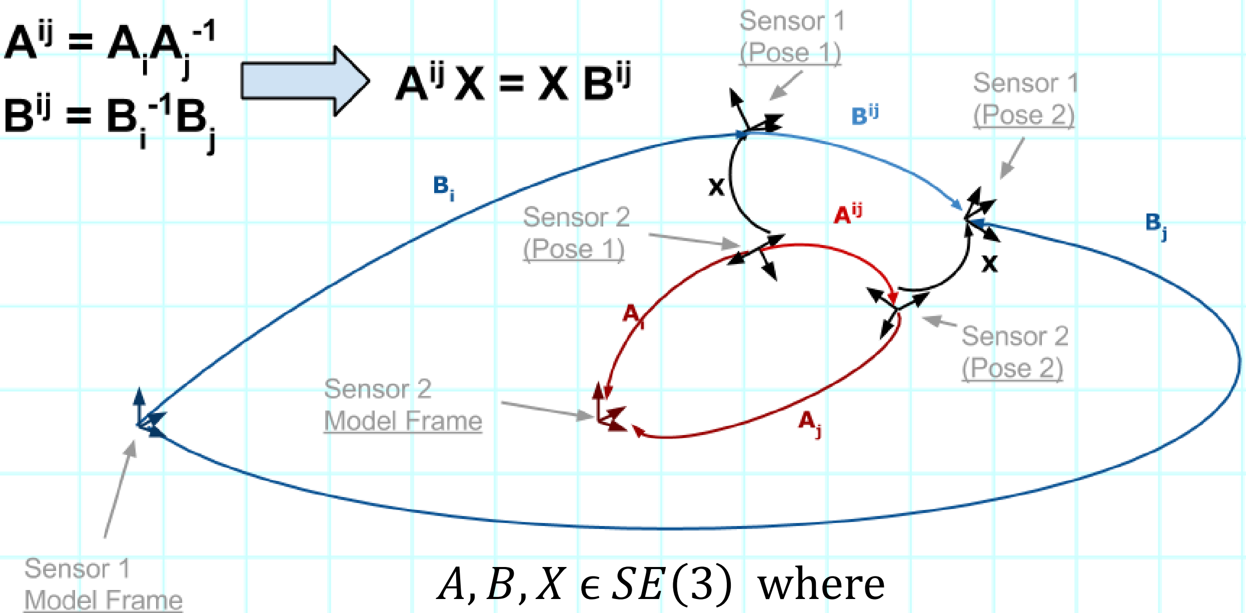

$$A, B, X \in SE(3) \text{ where}$$
$$\mathrm{SE}(3) = \mathbb{R}^3 \ltimes SO(3) \text{ and}$$
$$\mathrm{SO}(3) := \{R \in \mathbb{R}^{3x3} | RR^T = \mathbb{I}, \det(R) = +1\}$$

SE(3) is the Lie Group describing rigid body motions in 3-dimensional space, i.e.:

$H \in SE(3)$, where $H(R, \mathbf{t}) = \begin{pmatrix} R & \mathbf{t} \\ \mathbf{0}^T & 1 \end{pmatrix}$ and

$R \in SO(3)$ (a proper rotation matrix), $\mathbf{t} \in \mathbb{R}^3$ (a translation vector)

AX=XB Solution Space

It is well known that it is not possible to solve for a unique X from a single pair of exact (A, B),but if there are two instances of independent exact measurements, (A_1,B_1) and (A_2, B_2), then the problem can be solved.

$$AX = XB$$

$$\Downarrow$$

$$R_A R_X = R_X R_B \longrightarrow \text{One Parameter solution set}$$

+

$$\underbrace{(R_A - \mathbb{I}_3)}_{\text{Rank 2}} \mathbf{t}_X = R_X \mathbf{t}_B - \mathbf{t}_A$$

Rank 2

Two unspecified degrees of freedom

AX=XB Solution Space

A unique solution is possible given two pairs with certain constraints[4,5]

- SE(3) geometric invariants satisfied
- Angle of the rotation axes is "sufficiently large"
- *(A_i, B_i) pairs have Correspondence*

The goal becomes one of finding an X with least-squared error given corresponding pairs (A_i, B_i) for i=1,2,…,n.

[4] Chen (1991)
[5] Ackerman, M.K., Cheng, A., Shiffman, B., Boctor, E., Chirikjian, G. (2014)

AX=XB Correspondence

What we mean by correspondence:

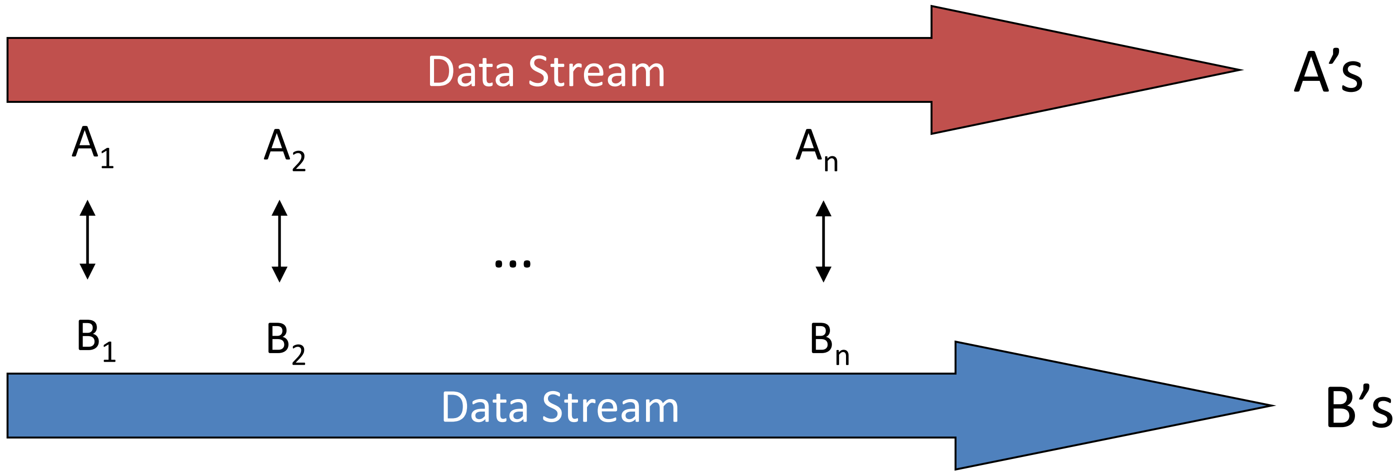

In experimental applications, it is often the case that the data streams containing the A’s and B’s:

- will present at different sample rates,
- will be asynchronous,
- and each stream may contain gaps in information.

AX=XB Correspondence

We present a method for calculating the calibration transformation, X, that works for data without any a priori knowledge of the correspondence between the A's and B's.

While our method removes the need to know the correspondence of the data, there have been other attempts in the literature to regenerate the correspondence by

1. time stamping the data[5]
2. dedicated software modules for syncing the data[6]
3. analyzing components of the sensor data stream to determine a correlation[7,8]

[5] Mills, D. L.

[6] Kang, H. J., Cheng, A., Boctor, E. M.

[7] Mair, E., Fleps, M., Suppa, M., Burschka, D

[8] Ackerman, M.,K., Cheng, A., Shiffman, B., Boctor, E., Chirikjian, G.

Rigid Body Motion

- The group of rigid body motions, $SE(3)$, $H \in SE(3)$, $H(R, \mathbf{t}) = \begin{pmatrix} R & \mathbf{t} \\ \mathbf{0}^T & 1 \end{pmatrix}$, where: $R = R_3(\alpha)R_1(\beta)R_3(\gamma)$, $\mathbf{t} = [t_x, t_y, t_z]^T$

is a Lie group and therefore the concept of integration exists:

$$\int_{SE(3)} f(H)\, dH = \int_{\mathbb{R}^3} \int_{SO(3)} f(H(R, \mathbf{t}))\, dR\, d\mathbf{t}$$

which is "natural", because for any $H_0 \in SE(3)$,

$$\int_{SE(3)} f(H) dH = \int_{SE(3)} f(H^{-1}) dH = \int_{SE(3)} f(HH_0) dH = \int_{SE(3)} f(H_0 H) dH$$

Convolution on $SE(3)$

Define the convolution of two functions as:

$$(f_1 * f_2)(H) = \int_{SE(3)} f_1(\mathcal{H}) f_2(\mathcal{H}^{-1} H) d\mathcal{H}$$

Define a delta function as:

$$\int_{SE(3)} \delta(H) dH = 1 \text{ and } (f * \delta)(H) = f(H).$$

And a shifted delta function as:

$\delta_A(H) = \delta(A^{-1}H)$, where $A \epsilon SE(3)$

The "v" operator is defined as:

$$\left(\sum_{i=1}^{n} x_i \tilde{E}_i\right)^{\vee} = (x_1, x_2, \ldots, x_n)^T$$

PDFs on *SE*(3)

The mean and covariance of a probability density function, *f*(*H*), can be defined as

$$\int_{SE(3)} \log(M^{-1}H) f(H)\, dH = \mathbb{O}$$

$$\Sigma = \int_{SE(3)} \log^{\vee}(M^{-1}H)[\log^{\vee}(M^{-1}H)]^T f(H)\, dH$$

Traditional Riemannian-geometric approach:

$$M' = \arg\min_{M} \int_{SE(3)} [d(M,H)]^2 f(H)\, dH$$

Wher $d(M,H)$ is usually s $d(M,H) = \|\log(M^{-1}H)\|_W^2$

Avoid the arbitrary bias of a weighting matrix and avoid the need for a bi-invariant distance metric, which does not exist for SE(3)

Mean and Covariance

- Traditional Riemannian-geometric approach:

$$M' = \arg\min_{M} \int_{SE(3)} [d(M,H)]^2 f(H)\, dH$$

Whe $d(M,H)$ is usually something akin to

$$d(M,H) = \|\log(M^{-1}H)\|_W^2$$

We use:

$$\int_{SE(3)} \log(M^{-1}H) f(H)\, dH = \mathbb{O}$$ and

$$\Sigma = \int_{SE(3)} \log^{\vee}(M^{-1}H)[\log^{\vee}(M^{-1}H)]^T f(H)\, dH$$

- *Avoid the arbitrary bias of a weighting matrix and avoid the need for a bi-invariant distance metric, which does not exist for SE(3)*

The "Batch" Equations

Give $\{A_i\}$ and $\{B_j\}$

$$A_i X = X B_i \Rightarrow \delta_{A_i}(H) = (\delta_X * \delta_{B_i} * \delta_{X^{-1}})(H)$$

because real-valued functions can be added and convolution is a linear operation on functions, all n instances can be written into a single eq $f_A(H) = (\delta_X * f_B * \delta_{X^{-1}})(H)$ where

$$f_A(H) = \frac{1}{n}\sum_{i=1}^{n} \delta(A_i^{-1}H) \text{ and } f_B(H) = \frac{1}{n}\sum_{i=1}^{n} \delta(B_i^{-1}H)$$

We can normalize the functions to be probability density functions (pdfs):

$$\int_{SE(3)} f_A(H)\,dH = \int_{SE(3)} f_B(H)\,dH = 1$$

The “Batch” Equations

Given th $d(A_i, A_j), d(B_i, B_j) < \epsilon << 1$, we can write the evolution of the mean and covariance as:

$$\boxed{M_{1*2} \approx M_1 M_2 \;\text{ and }\; \Sigma_{1*2} = Ad(M_2^{-1})\Sigma_1 Ad^T(M_2^{-1}) + \Sigma_2}$$

where

$$Ad(H) = \begin{pmatrix} R & \mathbb{O} \\ \hat{\mathbf{t}}R & R \end{pmatrix}$$

and the “hat” operator is defined such that given $\mathbf{a} \in \mathbb{R}^3$

$\hat{\mathbf{a}}\mathbf{b} = \mathbf{a} \times \mathbf{b}$ and $(\hat{\mathbf{a}})^\vee = \mathbf{a}$

The "Batch" Equations

Since the mean $\delta_X(H)$ is $M_X = X$ and its covariance is the zero matrix we can write the "Batch" formulation

$$\delta_{A_i}(H) = (\delta_X * \delta_{B_i} * \delta_{X^{-1}})(H)$$

$$f_A(H) = \frac{1}{n}\sum_{i=1}^{n}\delta(A_i^{-1}H) \text{ and } f_B(H) = \frac{1}{n}\sum_{i=1}^{n}\delta(B_i^{-1}H)$$

$$M_{1*2} = M_1 M_2 \text{ and } \Sigma_{1*2} = Ad(M_2^{-1})\Sigma_1 Ad^T(M_2^{-1}) + \Sigma_2$$

Batch Method "AX=XB" Equations:

(1) $\boxed{M_A = X M_B X^{-1}}$ (2) $\boxed{\Sigma_A = Ad(X)\Sigma_B Ad^T(X)}$

Solution Space

Batch Method "AX=XB" Equations:

(1) $\boxed{M_A = X M_B X^{-1}}$ (2) $\boxed{\Sigma_A = Ad(X)\Sigma_B Ad^T(X)}$

The search for an appropriate X can begin with re-writing (1 $\log^\vee(M_A) = Ad(X)\log^\vee(M_B)$

By defining

$$\log^\vee(M_A) = \begin{pmatrix} \theta_A \mathbf{n}_A \\ \mathbf{v}_A \end{pmatrix}$$

The equation can be separated into rotational and translational components,

$\mathbf{n}_A = R_X \mathbf{n}_B$ and $\mathbf{v}_A = \theta_B \widehat{\mathbf{t}_X} R_X \mathbf{n}_B + R_X \mathbf{v}_B$

From which it can be seen that the possible solution space, for (1), is two

Discretization

With the discrete nature of our application, we can likewise define the mean and covariance in

$$\sum_{i=1}^{n} \log(M_A^{-1}A_i) = \mathbb{O} \quad \text{and} \quad \Sigma_A = \frac{1}{n}\sum_{i=1}^{n} \log^{\vee}(M_A^{-1}A_i)[\log^{\vee}(M_A^{-1}A_i)]^T$$

An iterative procedure can be used for computing M_A which $M_A^0 = \exp(\frac{1}{n}\sum_{i=1}^{n}\log(A_i))$ estimate of the form

Then a gradient descent procedure is used to update so $C(M) = \|\sum_{i=1}^{n}\log(M^{-1}A_i)\|^2$ cost

The covariance can then be computed:

$$\Sigma_A = \frac{1}{n}\sum_{i=1}^{n} \log^{\vee}(M_A^{-1}A_i)[\log^{\vee}(M_A^{-1}A_i)]^T$$

Solution Space

For the rotational part, we can write R_X as

$R_X = R(\mathbf{n}_A, \mathbf{n}_B) R(\mathbf{n}_B, \phi)$ where $\phi \in [0, 2\pi)$ is the free parameter

We then re-write the translation part as

$$\frac{R(\mathbf{n}_A, \mathbf{n}_B) R(\mathbf{n}_B, \phi) \mathbf{v}_B - \mathbf{v}_A}{\theta_B} = \widehat{\mathbf{n}_A} \mathbf{t}_X$$

$\widehat{\boldsymbol{n}_A}$ is rank 2 so there is a degree of freedom in $\boldsymbol{t}_X$ along $\boldsymbol{n}_A$. Therefore we write $\boldsymbol{t}_X$ as

$$\mathbf{t}_X = \mathbf{t}(s) = s\,\mathbf{n}_A + a\,\mathbf{m}_A + b\,\mathbf{m}_A \times \mathbf{n}_A$$

Where $s \in \mathbb{R}$ is the free parameter and

$$\mathbf{m}_A \doteq \frac{1}{\sqrt{n_1^2 + n_2^2}} \begin{pmatrix} -n_2 \\ n_1 \\ 0 \end{pmatrix}$$

$$a = -\left(\frac{R(\mathbf{n}_A, \mathbf{n}_B) R(\mathbf{n}_B, \phi) \mathbf{v}_B - \mathbf{v}_A}{\theta_B} \right) \cdot (\mathbf{m}_A \times \mathbf{n}_A)$$

$$b = \left(\frac{R(\mathbf{n}_A, \mathbf{n}_B) R(\mathbf{n}_B, \phi) \mathbf{v}_B - \mathbf{v}_A}{\theta_B} \right) \cdot \mathbf{m}_A$$

Solution Space

A feasible solution to the batch equation can be parameterized as

$$X(\phi, s) = H(R(\mathbf{n}_A, \mathbf{n}_B)R(\mathbf{n}_B, \phi), \mathbf{t}(s))$$

where $(\phi, s) \in [0, 2\pi) \times \mathbb{R}$

Given that (1) constrains the possible solutions to a two-dimensional "cylinder", the problem of solving for X reduces to that of solving (2) on this cylinder by determining the values (ϕ, s). There is therefore no need to search elsewhere in the 6D group SE(3)

$||\cdot||_F^2$ Minimization

Minimize the cost function

$$\boxed{C_1(\phi, s) = \|Ad([X(\phi, s)]^{-1})\Sigma_A - \Sigma_B Ad^T(X(\phi, s))\|_F^2}$$

C_1 is quadratic in s and can be written as

$$C_1(\phi, s) = C_{10}(\phi) + C_{11}(\phi)s + \frac{1}{2}C_{12}(\phi)s^2$$

The minimization of s is solved for in closed-form,

$$s = -\frac{C_{11}(\phi)}{C_{12}(\phi)}$$

and then is substituted into the original expression, leaving $\phi \in [0, 2\pi)$

dimensional search over

KL Divergence

A Gaussian on $SE(3)$ can be defined when the norm $\|\Sigma\|$ is small as

$$\rho(H;M,\Sigma) = \frac{1}{(2\pi)^3|\Sigma|^{\frac{1}{2}}} e^{-\frac{1}{2}F(M^{-1}H)}$$

where $|\Sigma|$ denotes the determinant of Σ and

$$F(H) = [\log^{\vee}(H)]^T \Sigma^{-1} [\log^{\vee}(H)]$$

We write the Kullback-Leibler divergence of the two distributions as

$$D_{KL}(F_1 \| F_2) =$$

$$\frac{1}{2}\left[\mathrm{tr}(\Sigma_2^{-1}\Sigma_1) + (\mathbf{m}_2 - \mathbf{m}_1)^T \Sigma_2^{-1} (\mathbf{m}_2 - \mathbf{m}_1) - n - \ln\left(\frac{|\Sigma_1|}{|\Sigma_2|}\right)\right]$$

Minimal KL Divergence

Minimize the cost function

$$\boxed{C_2(X) = D_{KL}(f_A \,\|\, \delta_X * f_B * \delta_{X^{-1}})}$$

where

$f_A(H) = \rho(H; M_A, \Sigma_A)$ an

$$(\delta_X * f_B * \delta_{X^{-1}})(H) = \rho(H; XM_BX^{-1}, Ad(X)\Sigma_B Ad^T(X))$$

If we take into account that our search is limited to the cylinder as defined in (1), then automatically $XM_BX^{-1} = M_A$

Minimal KL Divergence

We can now write a new $K = M_A^{-1} H$,

, and minimize the cost function

$$C_2(X(\phi, s)) = D_{KL}(f'_A \,\|\, f'_B)$$

where $f'_A(K) = \rho(K; \mathbb{I}_4, \Sigma_A)$ an

$$f'_B(K) = \rho(K; \mathbb{I}_4, Ad(X(\phi, s))\Sigma_B Ad^T(X(\phi, s)))$$

Since SE(3) is unimodular, and additive and positive multiplicative constants can be ignored, we can simply consider the first term in the KL divergence, scaled by a fa

$$\boxed{C'_2(X(\phi, s)) = \mathrm{tr}(\Sigma_A^{-1} Ad(X(\phi, s))\Sigma_B Ad^T(X(\phi, s)))}$$

Minimal KL Divergence

- Since SE(3) is unimodular, and additive and positive multiplicative constants can be ignored, we can simply consider the first term in the K $C_2'(X(\phi,s)) = \mathrm{tr}(\Sigma_A^{-1} Ad(X(\phi,s)) \Sigma_B Ad^T(X(\phi,s)))$ of two minimized $(\phi, s) \in [0, 2\pi) \times \mathbb{R}$

- Minimization over s can be done in closed form as in the previous approach, since C_2 is also quadratic in s. After substit $\phi \in [0, 2\pi)$ his again

To experimentally test our methods for AX=XB calibration we use an Ultrasound (US) sensor calibration process. It should be noted that these methods can be extended to other application areas, both in US and more generally.

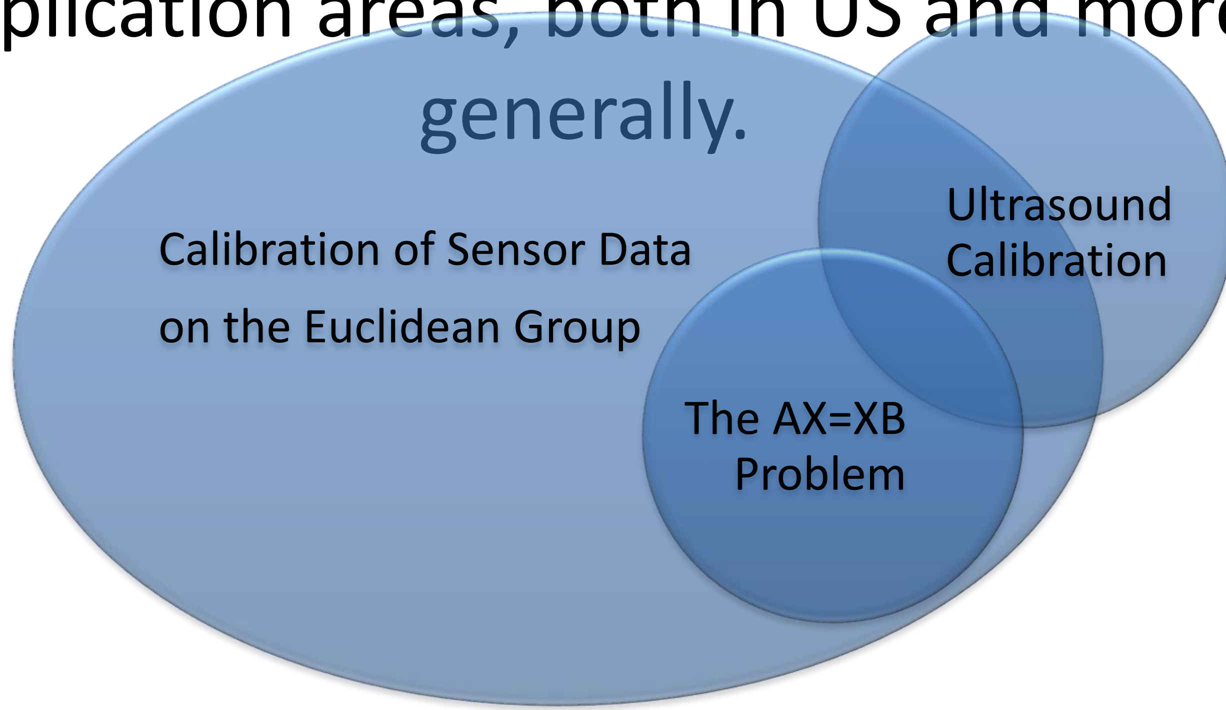

Through calibration we recover parameters that are required to perform more advanced forms of image based guidance using Ultrasound (US)

3D image volumes

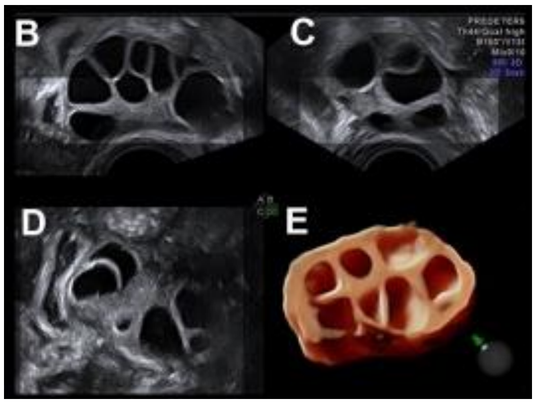

Augmented reality environments

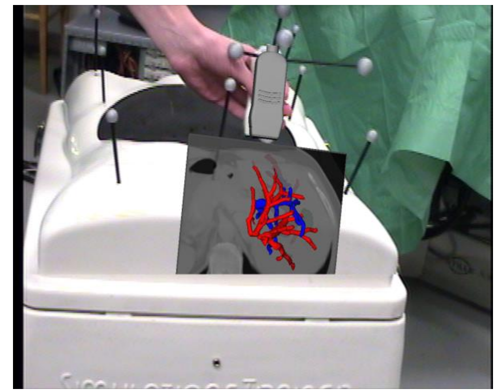

US Elastography

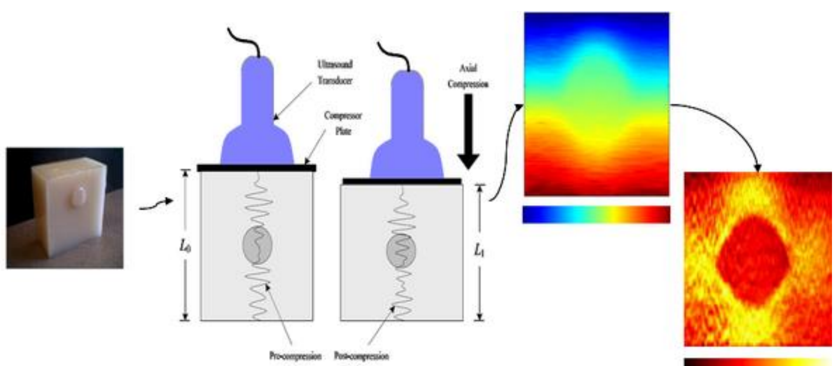

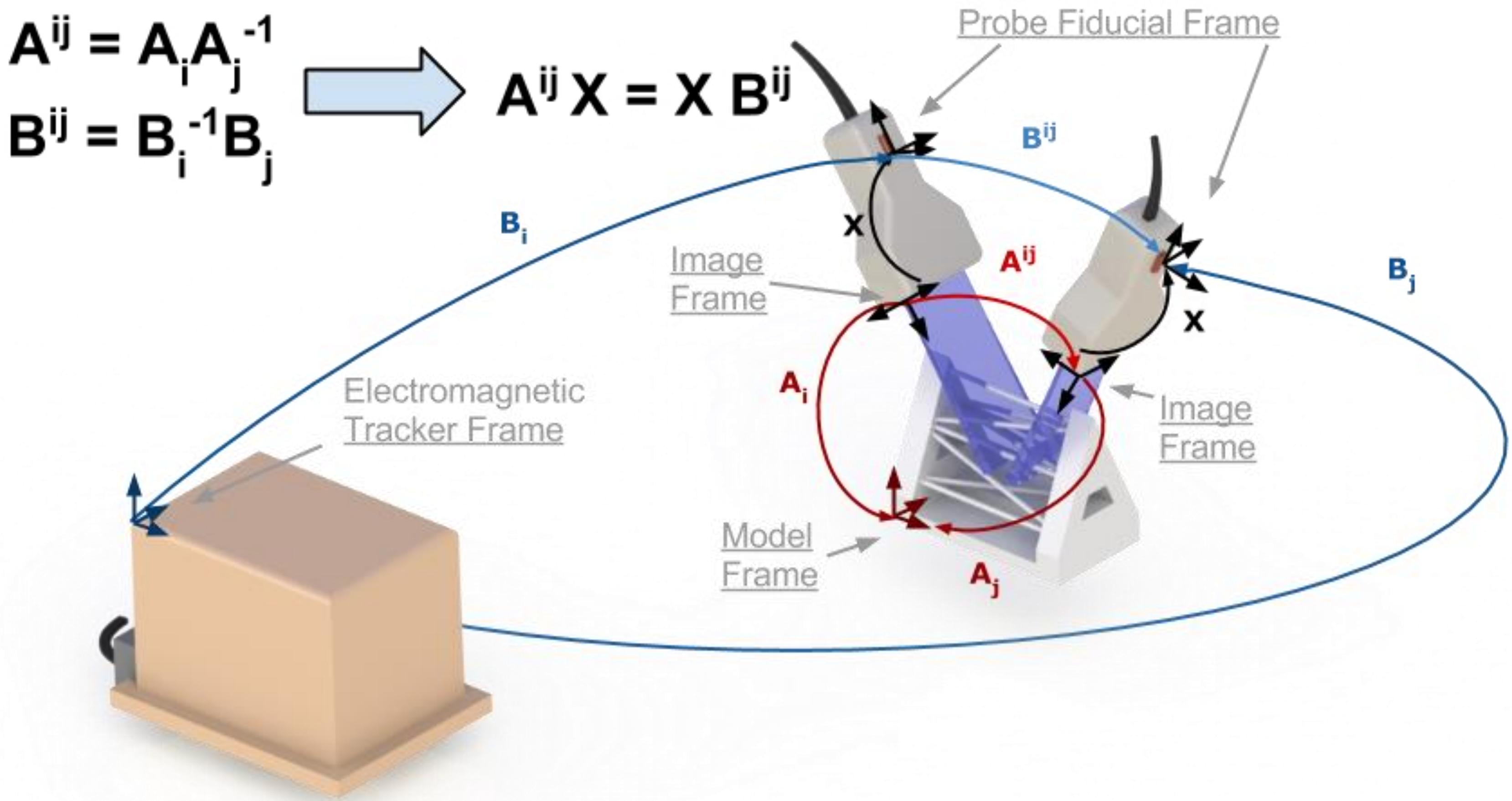

$A^{ij} = A_i A_j^{-1}$
$B^{ij} = B_i^{-1} B_j$
$A^{ij} X = X B^{ij}$
Probe Fiducial Frame
B^{ij}
B_i
X
Image Frame
A^{ij}
B_j
X
A_i
Electromagnetic Tracker Frame
Image Frame
Model Frame
A_j

Simulation Results

	Correspondence is Known	
	Rotation Error(rad)	Translation Error(mm)
KL	$1.4 \cdot 10^{-4}$	$1.4 \cdot 10^{-3}$
$\|\cdot\|_F^2$	$7.3 \cdot 10^{-4}$	$7.4 \cdot 10^{-3}$

	Correspondence is Unknown	
KL	$3.8 \cdot 10^{-4}$	$3.8 \cdot 10^{-3}$
$\|\cdot\|_F^2$	$7.3 \cdot 10^{-4}$	$7.4 \cdot 10^{-3}$

The two algorithms were unaffected by knowledge of correspondence and, in each case performed with a high level of accuracy. The results are the average of ten trials.

US Experimental Results

	Mean (mm)	Variance (mm)
KL	1.18	1.06
$\|\cdot\|_F^2$ Method	1.22	1.10

For each reconstruction point, we found its closest point match on the model and computed the sum squared difference between them. Our results show the mean and the standard deviation of this sum of squared differences and indicates that the error is reasonable.

US Experimental Results

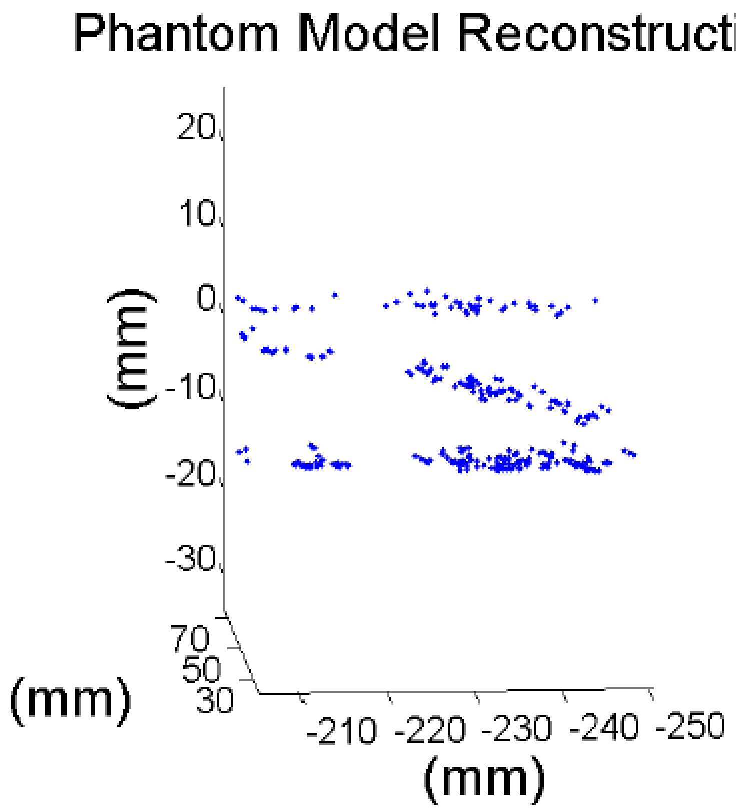

To examine the accuracy of the computed X, we performed a reconstruction of the phantom model.

Conclusions

- We established that the AX = XB sensor calibration problem can be formulated with a "Batch", probabilistic formulation that does not require a priori knowledge of the A and B correspondence.
- We presented an information-theoretic algorithm (KL Batch) that solves for X by minimizing the Kullback-Leibler divergence of the A and B sensor stream distributions with respect to the unknown X.
- In both simulation and experimentation, we demonstrated that this method reliably recovers an unknown X without the need for correspondence.

Future Work

- We will further examine the proposed methods experimentally, for ultrasound calibration, as well as other contexts.

- We will work to improve our probability theoretic formulation by specifically accounting for sensor measurement noise, representing X by a mean and covariance, and not just a Dirac delta distribution.

Acknowledgements

This work was supported by NSF Grant RI-Medium: 1162095

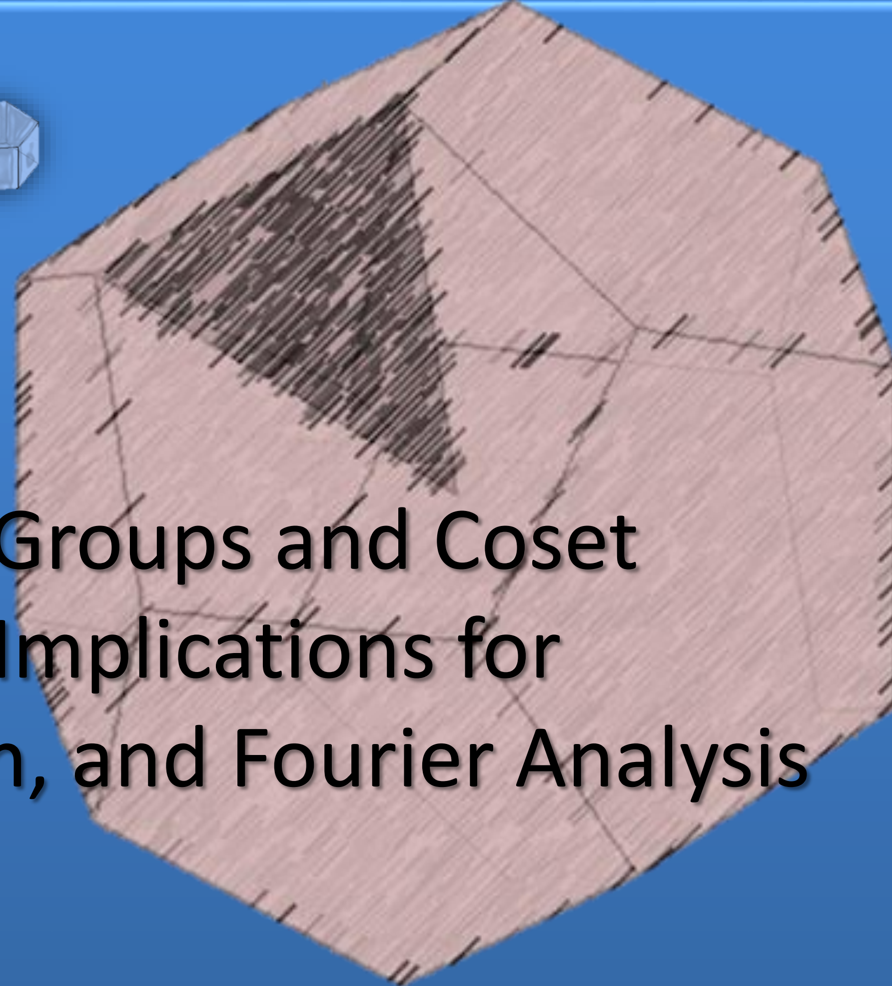

Voronoi Cells in Lie Groups and Coset Decompositions: Implications for Optimization, Integration, and Fourier Analysis

+

Yan Yan and Gregory S. Chirikjian

Department of Mechanical Engineering

Johns Hopkins University, Baltimore, MD 21218

Outlines

LABORATORY FOR Computational Sensing + Robotics THE JOHNS HOPKINS UNIVERSITY

- Review of basic concepts in group theory and the Lie groups SE(2) and SO(3).
- Generating almost-uniform sample points in SE(2)and SO(3) based on coset decomposition.
- More efficient computations of convolutions on groups developed by coset decomposition.

Basic concepts in group theory

- A group $(G,\circ)$ is a set, G, together with a binary operation, $\circ$,

that satisfies (1) closure; (2) associativity; (3) existence of identity element; (4) existence of inverse element.

In this paper, we mainly focus on the group of rotations in space, SO(3), and the group of rigid-body motions of the plane, SE(2).

- A subgroup is a subset of a group $(H \subseteq G)$ which is itself a group that is closed under the group operation of G.
- SO(3) and SE(2) contain discrete subgroups.

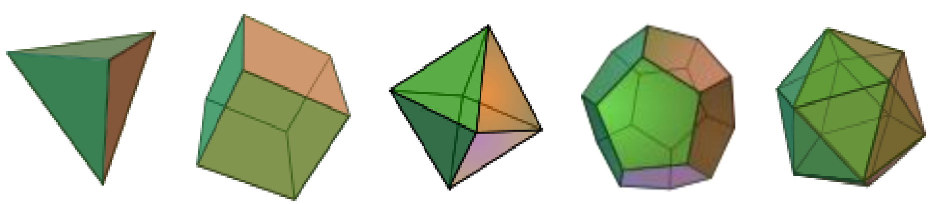

Groups of rotational symmetry operations of the Platonic solids

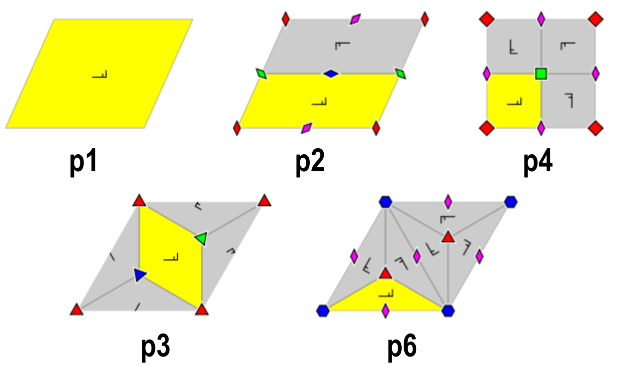

Five chiral wallpaper groups

Basic concepts in group theory

- Let $\Gamma, \Gamma' < G$ denote discrete subgroups, then left- and right- coset-spaces are defined as

$$G/\Gamma' \doteq \{g\Gamma' \mid g \in G\} \text{ and } \Gamma\backslash G \doteq \{\Gamma g \mid g \in G\}.$$

A double coset space is define as $\Gamma\backslash G/\Gamma' \doteq \{\Gamma g \Gamma' \mid g \in G\}.$

- Associated with any (double-) coset, it is possible to define a fundamental domain in G, which is a set of distinguished (double-) coset representatives, exactly one per (double-) coset. It has the same dimension as G, but lesser volume.
- It can be constructed as Voronoi cells in G.

$$F_{\Gamma\backslash G} \doteq \{g \in G \mid d(e,g) < d(e,\gamma\circ g)\ ,\forall\, \gamma \in \Gamma\}$$

$$F_{G/\Gamma'} \doteq \{g \in G \mid d(e,g) < d(e,\gamma'\circ g)\ ,\forall\, \gamma' \in \Gamma'\}$$

and when $\Gamma \cap \Gamma' = \{e\}$, $F_{\Gamma\backslash G/\Gamma'} \doteq \{g \in G \mid d(e,g) < d(e,\gamma\circ g\circ\gamma')\ ,\forall\, (\gamma,\gamma') \in \Gamma\times\Gamma'\}.$

Fundamental domains for SO(3)

- Constructed as Voronoi cells with $d_{SO(3)}(R_1, R_2) = \| \log(R_1^T R_2) \|$

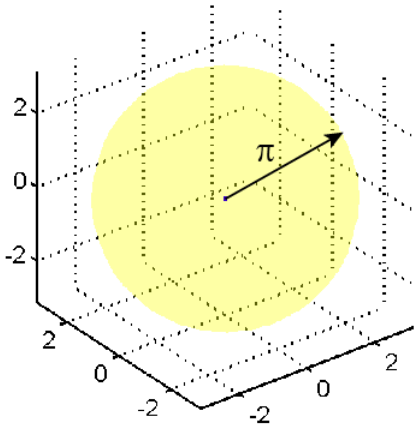

SO(3) represented in exponential coordinates

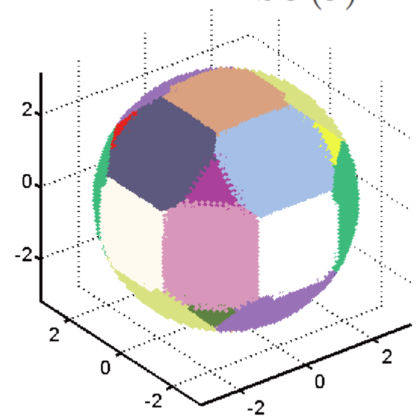

Voronoi cells
Γ: the Icosahedral group

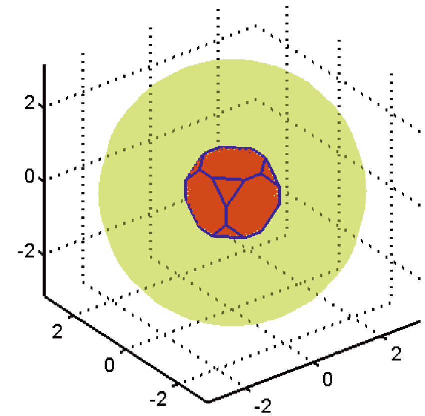

The center Voronoi cell
⇔ the fundamental domain

- Fundamental domain for other discrete subgroups in SO(3):

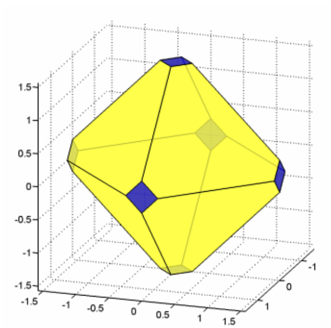

The Tetrahedral group

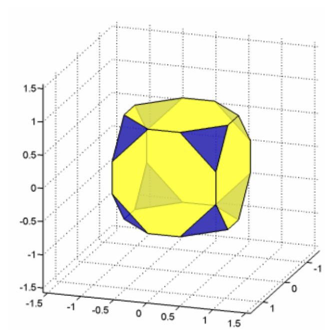

The Octahedral group

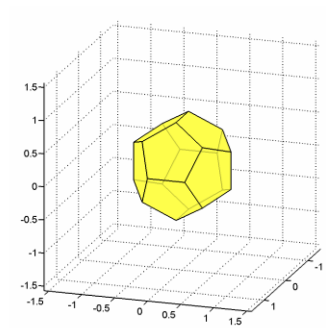

The Icosahedral group

Smallest volume!

(Yan and Chirikjian, ICRA'12)

Fundamental domains for SE(2)

LABORATORY FOR
Computational Sensing + Robotics
THE JOHNS HOPKINS UNIVERSITY

- For the first time, we establish the fundamental domains for SE(2) when Γ is one of the five chiral wallpaper groups, p1, p2, p3, p4 and p5.
- Distance function: $d_{SE(2)}(g_1, g_2) = \| \log(g_1^{-1} \circ g_2) \|_W$

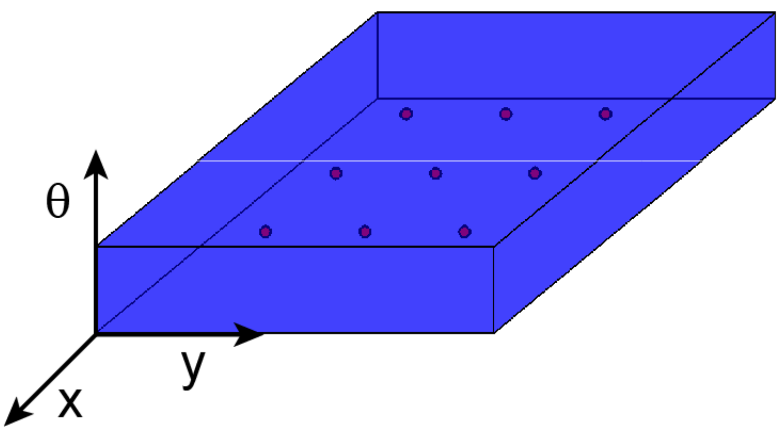

SE(2) represented in $\mathbb{R}^3$

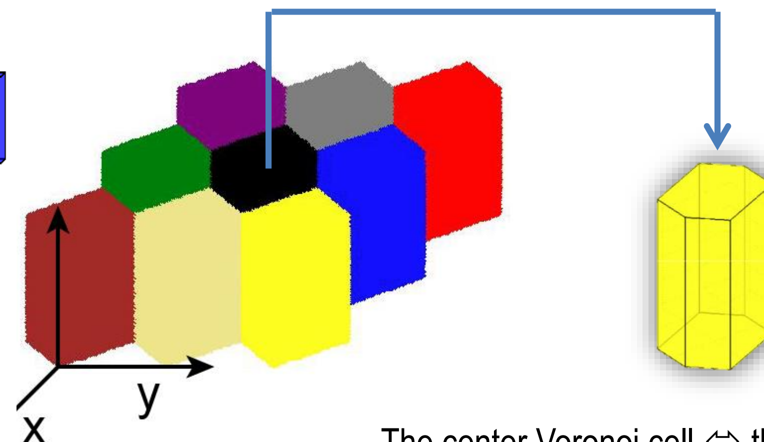

Voronoi cells with $\Gamma = \mathbf{p1}$

The center Voronoi cell ⇔ the fundamental domain
For **p1**: it looks like a hexagonal box with the height from –π to π.
We note that if the lattice is square instead of parallelogrammatic, the center Voronoi cells becomes a square box.

Fundamental domains for SE(2)

LABORATORY FOR Computational Sensing + Robotics
THE JOHNS HOPKINS UNIVERSITY

- Fundamental domains of SE(2) based on the five chiral wallpaper groups:

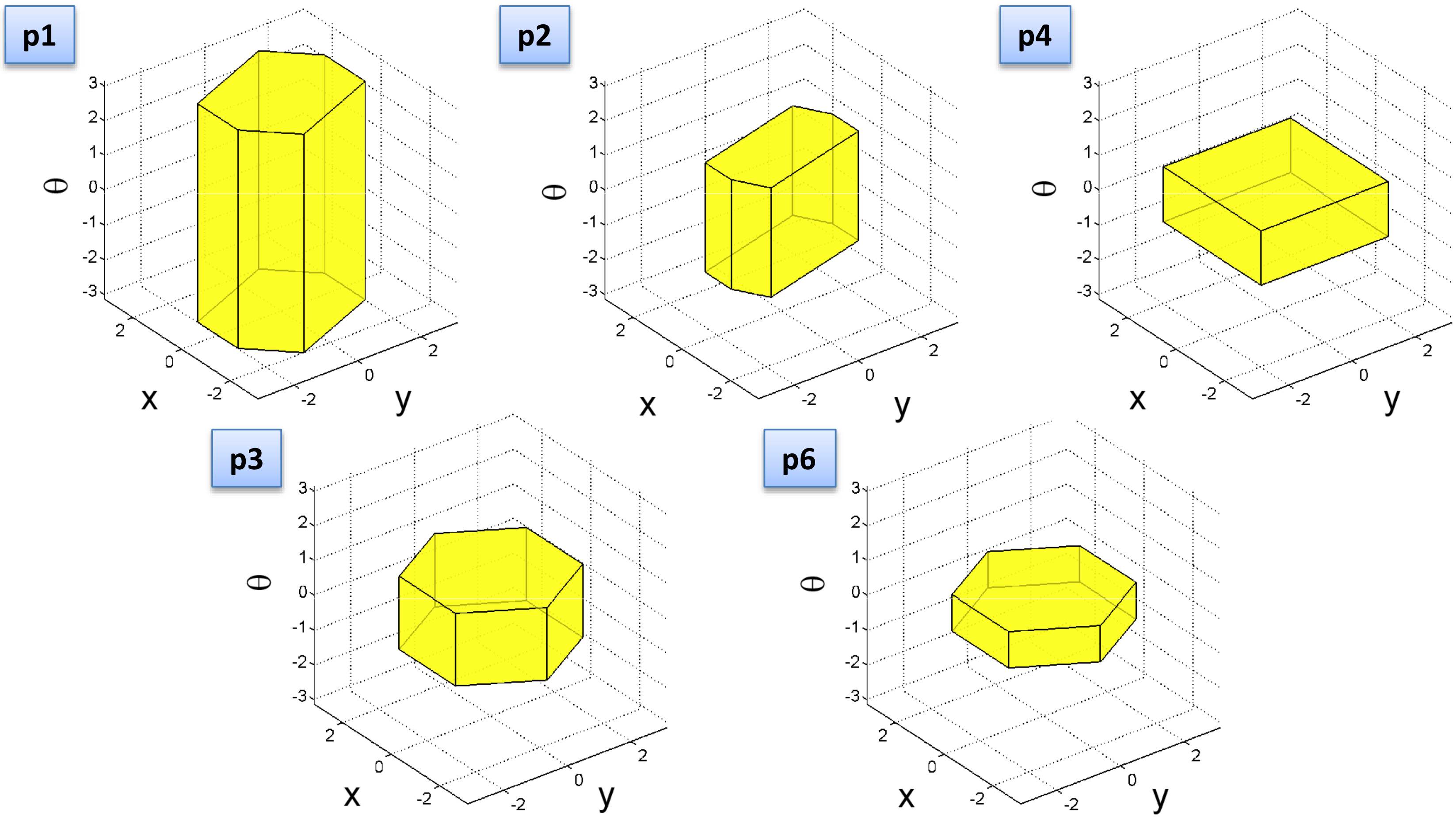

Why do we study this?

Application 1:
generating almost-uniform samples

Importance of uniform sampling

- The discretization of the groups of rotations or rigid-body motions, arises in many applications such as
  - robot motion planning;
  - computational structural biology;
  - Computer graphics

- Uniform sampling will prevent search algorithms from oversampling or undersampling large portions of the C-space.
- This affects both the performance and reliability of planning algorithms.

Sampling based on single coset decomposition

SO(3) Example:

$$R = \exp(\hat{\mathbf{n}}\theta), \quad \exp\hat{\mathbf{x}} \approx \mathbb{I} + \hat{\mathbf{x}} \text{ when } ||\mathbf{x}|| \text{ is small}$$

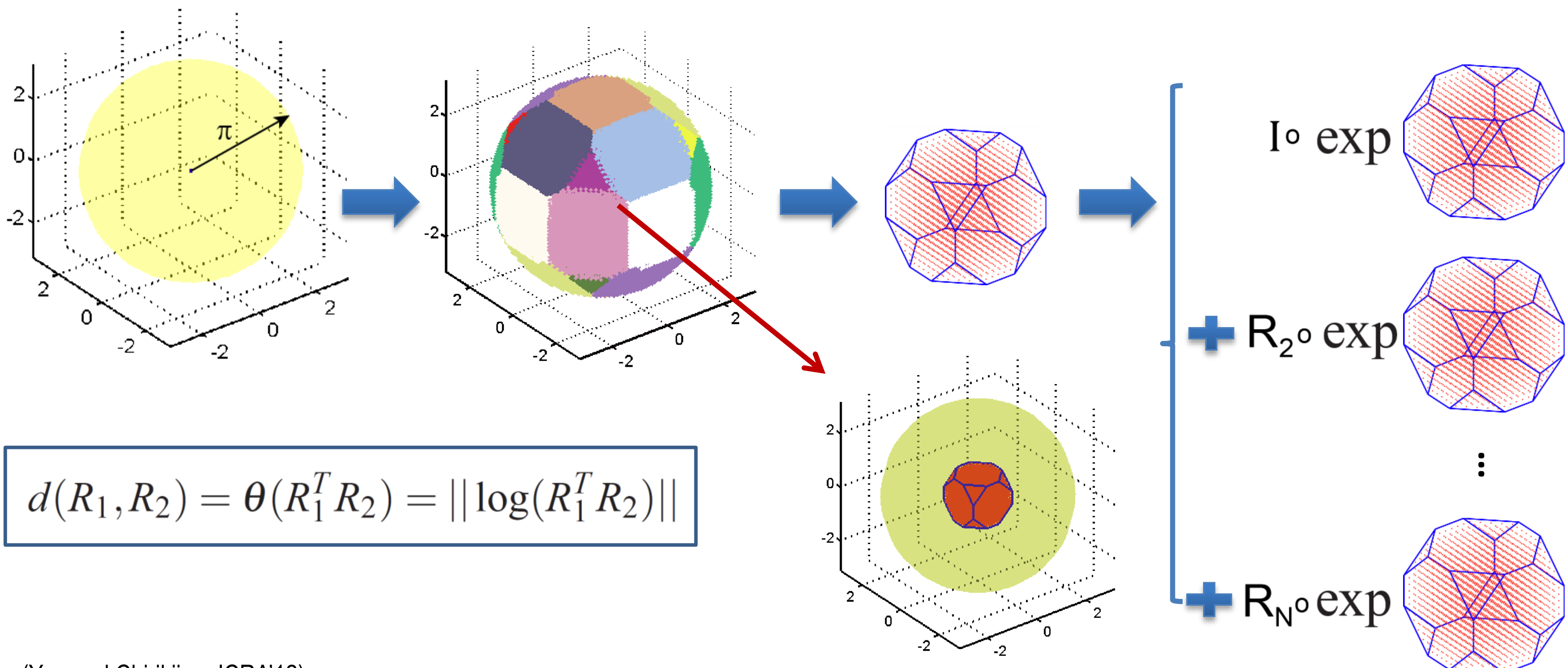

$$\boxed{d(R_1, R_2) = \theta(R_1^T R_2) = ||\log(R_1^T R_2)||}$$

(Yan and Chirikjian, ICRA'12)

Sampling based on single coset decomposition

Distortion measure: $\boxed{C(\mathbf{q}) = \frac{1}{\sqrt{3}}\|G(\mathbf{q}) - \mathbb{I}\|}$ where $G(\mathbf{q}) = J^T(\mathbf{q})J(\mathbf{q})$

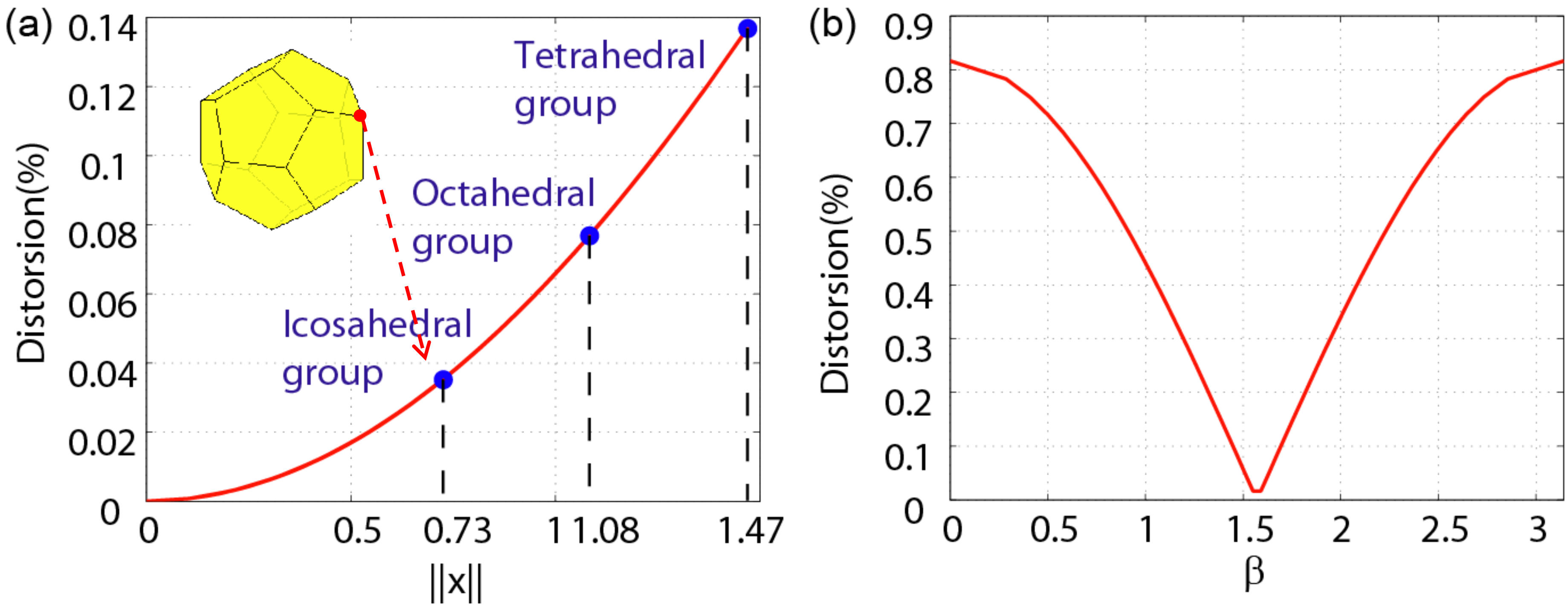

our sampling method

ZXZ Euler angles

The grids generated on SO(3) are almost uniform!

Can we do better than this?

Sampling based on double coset decomposition

LABORATORY FOR Computational Sensing + Robotics
THE JOHNS HOPKINS UNIVERSITY

- Given two finite subgroups, $H, K < G$, where $G = SO(3)$, $|H \cap K| = 1$, the resulting non-overlapping tiles satisfy

$$G = \bigcup_{h \in H} \bigcup_{k \in K} h \overline{F_{H \backslash G / K}} k^{-1}.$$

- Some examples of double-coset spaces:

(a) H=tetrahedral group (conjugated), K= icosahedral group (b) H=octahedral group (conjugated), K= icosahedral group (c) H=icosahedral group (conjugated), K= icosahedral group

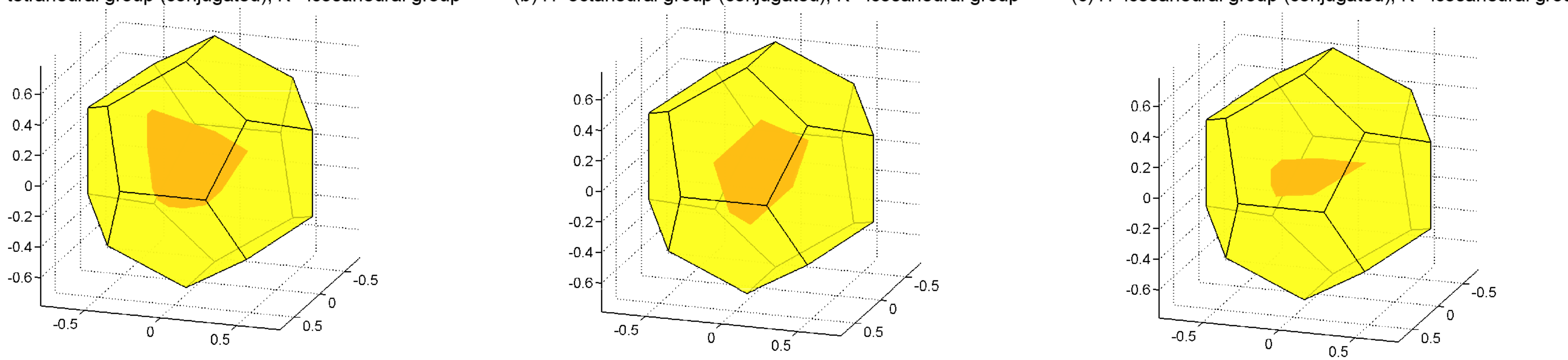

Yellow-shaded region: single coset-space $F_{SO(3)/K}$ with K= the icosahedral group

Red-shaded region: double coset-space $F_{H \backslash SO(3)/K}$ with K= the icosahedral group, H= the conjugated (a) tetrahedral , (b) octahedral, and (c) icosahedral groups. The conjugated group H: $H = gH_0g^{-1}$ for $g \in G$.

Sampling based on double coset decomposition

LABORATORY FOR Computational Sensing + Robotics THE JOHNS HOPKINS UNIVERSITY

As $|H| \cdot |K|$ increases, the size of the center Voronoi cells shrinks, which leads to smaller distortion.

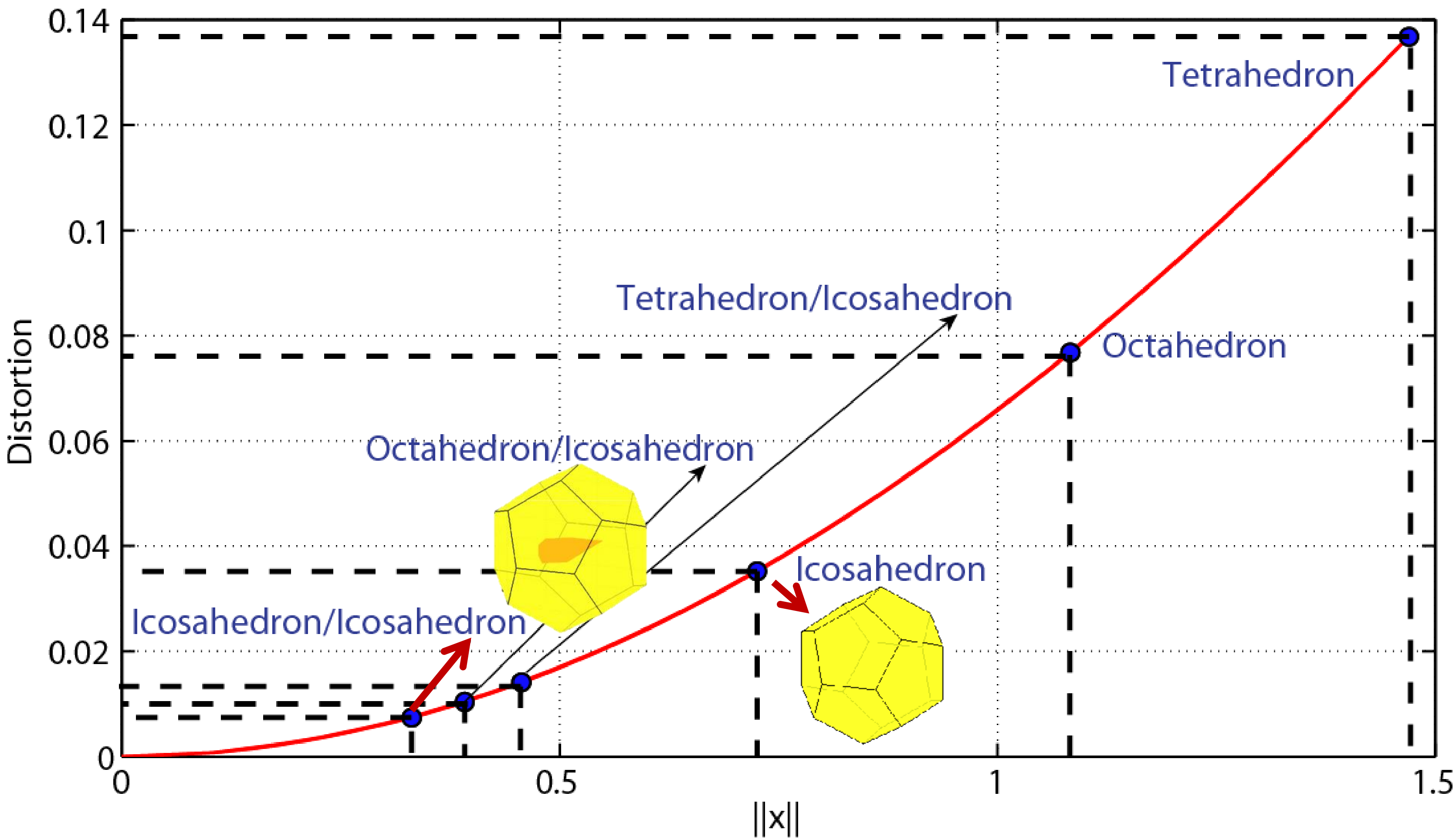

Advantages of this sampling approach?

- has low metric distortion
- is deterministic
- has grid structure with respect to the metric on SO(3)
- can easily achieve any level of resolution

Application 2:
Efficient computation of convolution on rotation and motion groups

Fast Convolutions by Direct Evaluation

- Convolution on groups: $(f_1 * f_2)(g) = \int_G f_1(h) f_2(h^{-1} \circ g) dh$

Here, dh is the natural integration measure for G.

- Efficient algorithms for computing convolutions on roation and motion groups have been developed previously using “group FFTs” --- Chirikjian and Kyatkin, 01; Kostelec and Rockmore, 08; Maslen and Rockmore, 97.
- Usually Euler angle decompositions are used for SO(3).
- We introduce two potential alternatives to this approach based on double coset decompositions described earlier.

- Computed by direct evaluation:

An integration over G : $\int_G f(g) dg = \sum_{(h,k) \in H \times K} \int_{F_{H \backslash G/K}} f(h \circ g' \circ k) dg'$

where dg' is the same volume element as for G, but restricted to $F_{H \backslash G/K} < G$.

Fast Approximate FFTs on SO(3) and SE(2)

- Instead of using Euler angles to parameterize *SO*(3), we can develop different FFT algorithms based on different parameterizations and coset decompositions.

- Specific property of IURs (irreducible unitary representations)

$$U(\exp X, l) = \exp(W(X,l))$$

where $W(X,l) = \sum_{i=1}^{3} x_i W_i(l)$ with

$$(W_1(l))_{mn} = -\frac{i}{2}c_{-n}^{l}\delta_{m+1,n} - \frac{i}{2}c_{n}^{l}\delta_{m-1,n}$$

$$(W_2(l))_{mn} = +\frac{i}{2}c_{-n}^{l}\delta_{m+1,n} - \frac{i}{2}c_{n}^{l}\delta_{m-1,n}$$

$$(W_3(l))_{mn} = -in\delta_{m,n}$$

- The fact that on the fundamental domain centered on the identity $U(expX, l)$ can be expressed as a truncated Taylor series in X is then very useful because $W(X,l)$ will have polynomial entries, each of which can be computed by evaluation on their boundary.
- Therefore, the computation of the integral over $F_{H\backslash SO(3)/K}$ is efficient.

- We use this property together with the double coset decomposition:

$$\hat{f}(l) = \sum_{(P,Q)\in\mathbb{P}\times\mathbb{Q}} \int_{F_{\mathbb{P}\backslash SO(3)/\mathbb{Q}}} f(PRQ)U((PRQ)^T,l)dR, \quad \Leftrightarrow \quad \sum_{(P,Q)\in\mathbb{P}\times\mathbb{Q}} U(Q^T,l)\left[\int_{F_{\mathbb{P}\backslash SO(3)/\mathbb{Q}}} f(PRQ)U(R^T,l)dR\right]U(P^T,l)$$

where $\mathbb{P},\mathbb{Q} < SO(3)$ are finite.

Conclusions (for this part)

- We make a connection between Voronoi cells in the groups SO(3) and SE(2) centered on elements of discrete subgroups, and coset- and double-coset-spaces.
- We show that sampling within these Voronoi cells can be made almost uniform by exponentiating a Cartesian grid in a region of the corresponding Lie algebra, which is the pre-image of these cells under the exponential map.
- We show how the resulting cells, and the samples therein, can be used for searches, optimization, and Fourier analysis on certain Lie groups of interest in robotics and control.

DETC2014-34243

KINEMATICS MEETS CRYSTALLOGRAPHY: THE CONCEPT OF A MOTION SPACE

Gregory S. Chirikjian
Robot and Protein Kinematics Lab
Department of Mechanical Engineering
Johns Hopkins University
Baltimore, MD 21218, USA

First Some Pretty Pictures from Old Work: Elastic Network Interpolation for the GroEL-GroES complex

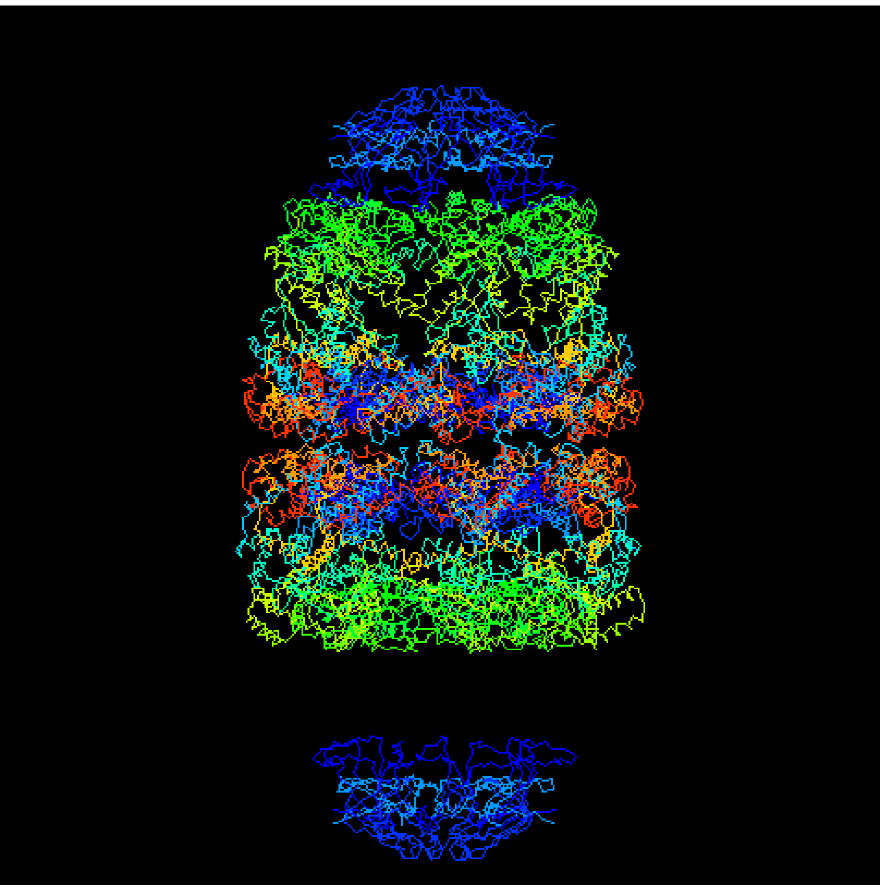 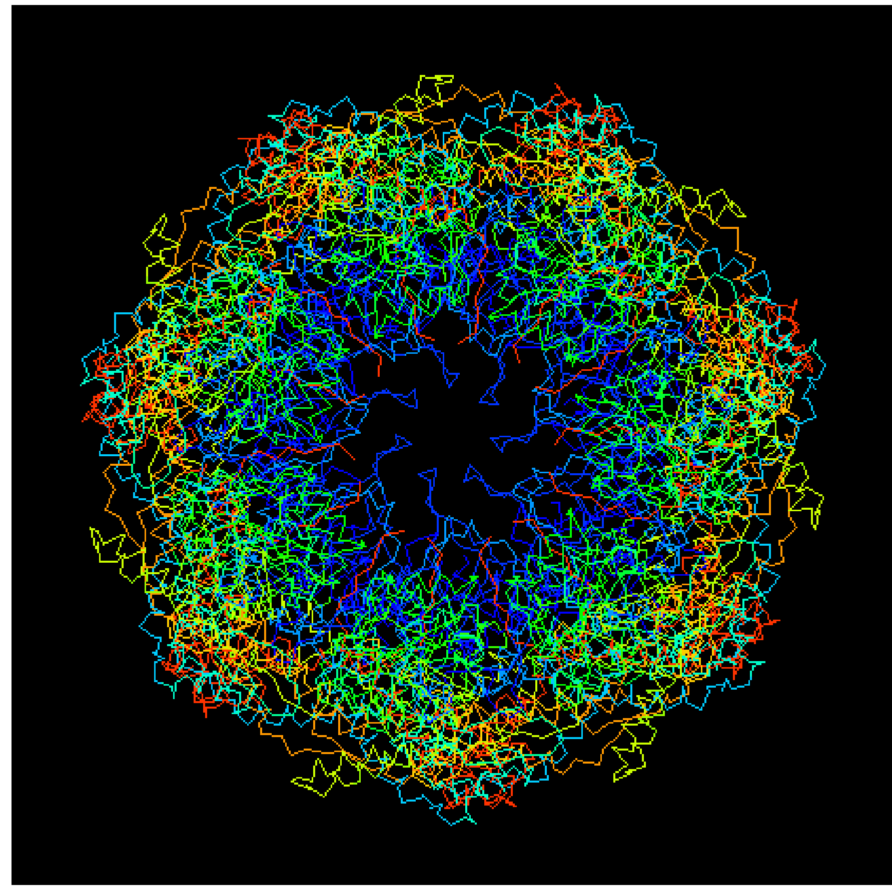

What is the Structure of the Space of Motions of Bodies that Move Collectively with Symmetry ?

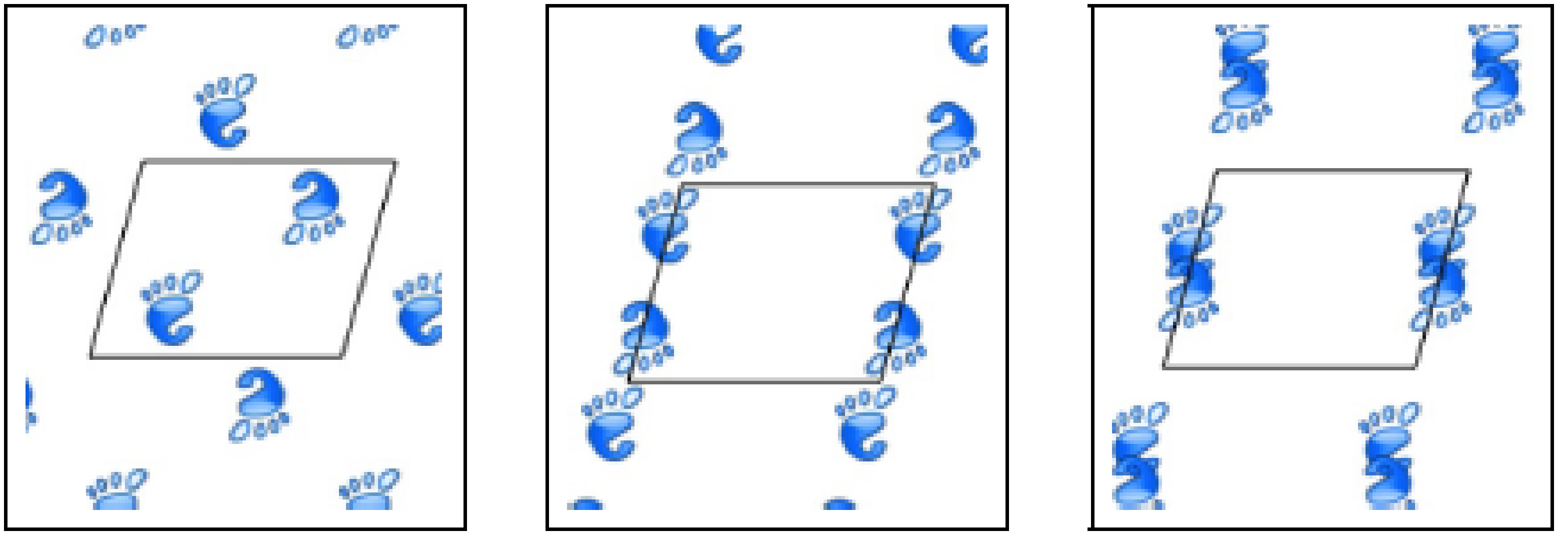

(a) (b) (c)

Fig. 1. Three configurations of solid bodies with $p2$ symmetry

Figure generated using ``Escher Mobile iphone App”
developed in the group of G. Chapuis at EPFL

How to Characterize the Free Space of Motions of Bodies that Move Collectively with Symmetry ?

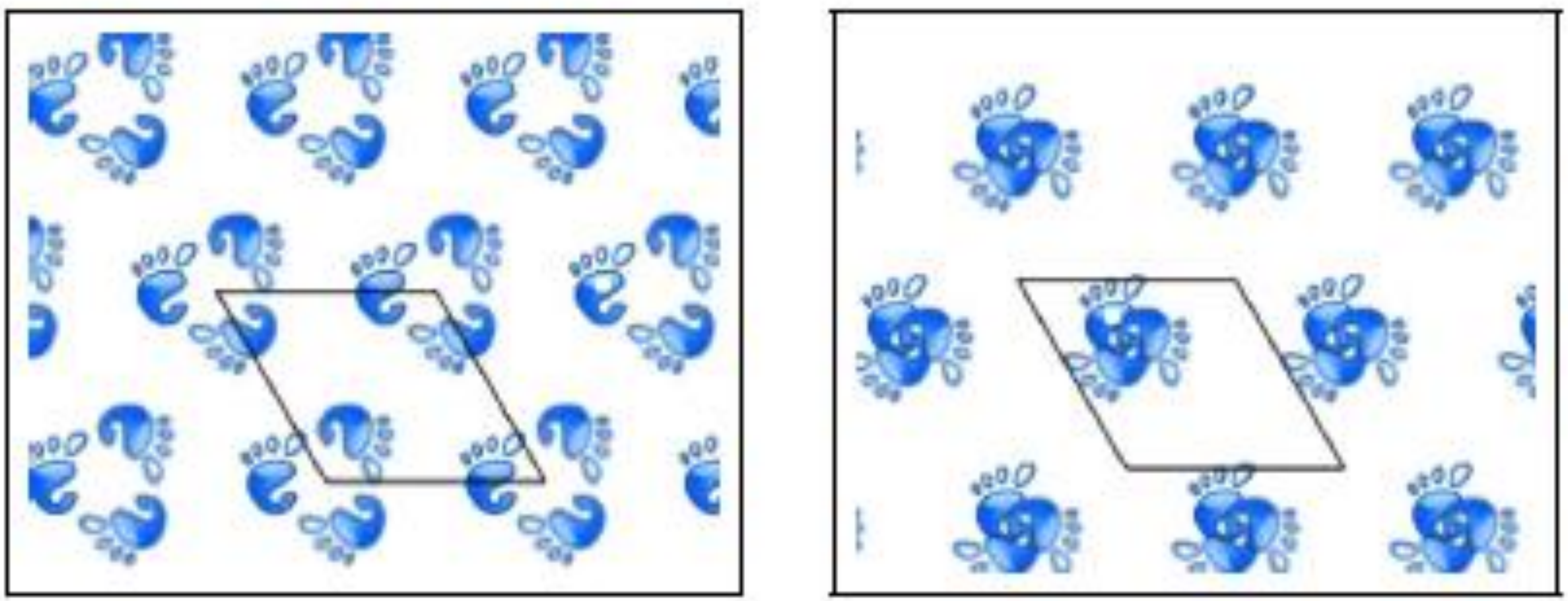

(a) (b)

Fig. 2. Two configurations of solid bodies with $p3$ symmetry

Protein X-Ray Crystallography

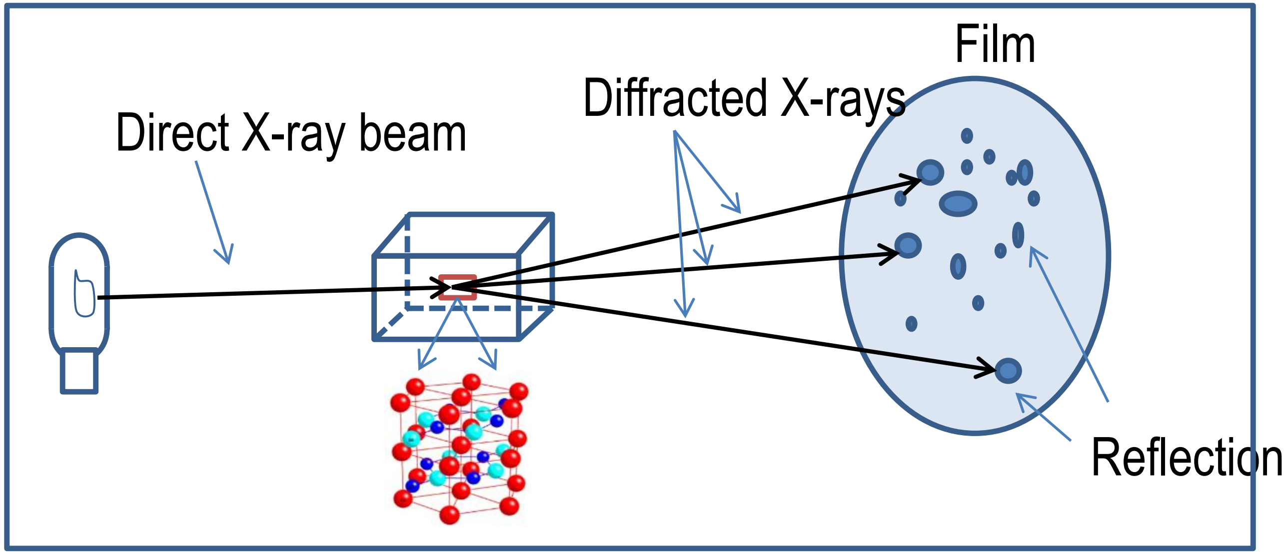

Electron density of a single-protein: $$f(\mathbf{x}) = \sum_{i=1}^{n} \rho_i(\mathbf{x} - \mathbf{x}_i)$$

$\mathbf{x}_i = (x_i, y_i, z_i)$: the Cartesian coordinates of the i-th atoms;

$\rho_i(\mathbf{x})$:the electron density map of i-th atom in a reference frame centered on it.

Diffraction pattern from X-ray crystallography experiment:

$$\hat{P}(g;\vec{k}) = \left| \mathscr{F}\left(\sum_{j=1}^{m} f\left((\gamma_j \circ g)^{-1} \cdot \vec{x}\right) \right) \right|$$

$f(\vec{x})$:electron density of a single protein; $\mathscr{F}(\cdot)$ ier transform;

$\{\gamma_j\}$:crystal symmetry operation (known); : g d-body motion (unknown).

X Shorthand for $\mathbb{R}^n$ (parameterized in Cartesian coordinates $\{x_i\}$).

$SE(n)$ The special Euclidean group of n-dimensional space.

G Shorthand for $SE(3)$, a six-dimensional Lie group.

Γ A chiral crystallographic space group.

$\mathbb{L}$ A lattice in Euclidean space.

T The discrete group of translational symmetries of a lattice.

$\mathbb{F}$ The factor group $\Gamma/T = T\backslash\Gamma$.

$\mathbb{T}^n$ The n-dimensional torus.

$F_{\Gamma\backslash G}$ The fundamental domain in G corresponding to $\Gamma\backslash G$.

$\mathbb{Z}$ The integers

Symmetries in the Density Function of a Protein Crystal

$$\rho_{\Gamma\backslash X}(\mathbf{x}) \doteq \sum_{\gamma \in \Gamma} \rho(\gamma^{-1} \cdot \mathbf{x}).$$

$$\rho_{\Gamma\backslash X}(\gamma_0^{-1} \cdot \mathbf{x}) = \rho_{\Gamma\backslash X}(\mathbf{x}).$$

Rigid-Body Motions in Euclidean Space

$$SE(n) = (\mathbb{R}^n, +) \rtimes SO(n)$$

$$g_1 \circ g_2 = (R_1, \mathbf{t}_1) \circ (R_2, \mathbf{t}_2) = (R_1 R_2, R_1 \mathbf{t}_2 + \mathbf{t}_1)$$

$$g^{-1} = (R^T, -R^T \mathbf{t}) \quad \text{and} \quad e = (\mathbb{I}, \mathbf{0})$$

$$\mathcal{T} = \{(\mathbb{I}, \mathbf{t}) \mid \mathbf{t} \in X\} \quad \text{and} \quad \mathcal{R} = \{(R, \mathbf{0}) \mid R \in SO(n)\}$$

Decomposing Continuous Motions

$$\mathrm{screw}(\mathbf{n}, \theta, h) = \begin{pmatrix} e^{\theta N} & h\mathbf{n} \\ \mathbf{0}^T & 1 \end{pmatrix}$$

$$\mathcal{T} = \{(\mathbb{I}, \mathbf{t}) \mid \mathbf{t} \in X\} \quad \text{and} \quad \mathcal{R} = \{(R, \mathbf{0}) \mid R \in SO(n)\}$$

$$(R, \mathbf{0}) \circ \mathrm{screw}(\mathbf{n}, \theta, h) \circ (R^T, \mathbf{0}) = \mathrm{screw}(R\mathbf{n}, \theta, h)$$

Discrete (Crystallographic) Motion Groups

Though continuous screw motions (both infinitesimal and finite) are known to kinematicians, discrete screw motions are important in crystallography. In the case when $\theta = 2\pi/\eta$ and $h = p/\eta$, where p and η are positive integers and $p \in \{1, 2, ..., \eta\}$, $\text{screw}(\mathbf{n}, 2\pi/\eta, p/\eta)$ becomes a screw axis of type η_p, where

$$[\text{screw}(\mathbf{n}, 2\pi/\eta, p/\eta)]^\eta = (\mathbb{I}, p\mathbf{n}).$$

If we conjugate by translations before raising to the power, the result is the same because

$$[(\mathbb{I}, \mathbf{t}) \circ \text{screw}(\mathbf{n}, 2\pi/\eta, p/\eta) \circ (\mathbb{I}, -\mathbf{t})]^\eta =$$
$$(\mathbb{I}, \mathbf{t}) \circ (\mathbb{I}, p\mathbf{n}) \circ (\mathbb{I}, -\mathbf{t}) = (\mathbb{I}, p\mathbf{n}).$$

Examples of Crystallographic Space Groups

(case 1) $P_{2_12_12_1}$: (x,y,z); (-x+1/2,-y,z+1/2); (-x,y+1/2,-z+1/2); (x+1/2,-y+1/2,-z);

(case 2) P_{2_1} : (x,y,z); (-x,y+1/2,-z);

(case 3) C_2 : (x,y,z); (-x,y,-z); (x+1/2,y+1/2,z); (-x+1/2,y+1/2,-z);

(case 4) $P_{2_12_12}$: (x,y,z); (-x,-y,z); (-x+1/2,y+1/2,-z); (x+1/2,-y+1/2,-z);

(case 5) C_{222_1} : (x,y,z); (-x,-y,z+1/2); (-x,y,-z+1/2); (x,-y,-z); (x+1/2,y+1/2,z);
(-x+1/2,-y+1/2,z+1/2); (-x+1/2,y+1/2,-z+1/2); (x+1/2,-y+1/2,-z);

(case 6) $P_{4_32_12}$: (x,y,z); (-x,-y,z+1/2); (-y+1/2,x+1/2,z+3/4); (y+1/2,-x+1/2,z+1/4); (-x+1/2,y+1/2,-z+3/4); (x+1/2,-y+1/2,-z+1/4); (y,x,-z); (-y,-x,-z+1/2); The value of $|P_u|\setminus|S|$ in these six cases are respectively 3, 1,1, 1, 3, and 3.

Cosets, Quotients, and Fundamental Domains

$$F_{\Gamma\backslash G} \cong \left(F_{\Gamma\backslash X}\right) \times SO(3).$$

$$F_{\Gamma_s\backslash G} = \left(F_{T\backslash X}\right) \times \left(F_{P_s\backslash SO(3)}\right)$$

Concrete Planar Examples

$$H(g(x,y,\theta)) = \begin{pmatrix} \cos\theta & -\sin\theta & x \\ \sin\theta & \cos\theta & y \\ 0 & 0 & 1 \end{pmatrix}$$

$$p1 = \{g(z_1, z_2, 0) \,|\, z_1, z_2 \in \mathbb{Z}\}$$

$$F_{p1\backslash SE(2)} = \{(x, y, \theta) \in [0,1) \times [0,1) \times [0, 2\pi)\}$$

p4 = $\{g(z_1, z_2, k\pi/2) \,|\, z_1, z_2 \in \mathbb{Z}, k \in \{0,1,2,3\}\}$

$$\overline{F_{p4\backslash SE(2)}} \cong \{(x, y, \theta) \in [0, 1/2] \times [0, 1/2] \times [0, 2\pi]\}$$

Embeddings and Immersions of Motion Spaces in R^n

$$y = y(g(x, y, \theta))$$

$$y(\gamma \circ g(x, y, \theta)) = y(g(x, y, \theta))$$

p1\SE(2) = T^3

$$\begin{aligned} y_1 &= \cos(2\pi x) \\ y_2 &= \sin(2\pi x) \\ y_3 &= \cos(2\pi y) \\ y_4 &= \sin(2\pi y) \\ y_5 &= \cos\theta \\ y_6 &= \sin\theta\,. \end{aligned}$$

Immersions of p4\SE(2) in R^6

$$
\begin{aligned}
(x, y, \theta) &\to (x + z_1, y + z_2, \theta), \\
(x, y, \theta) &\to (-y + z_1, x + z_2, \theta + \pi/2), \\
(x, y, \theta) &\to (-x + z_1, -y + z_2, \theta + \pi), \\
(x, y, \theta) &\to (y + z_1, -x + z_2, \theta + 3\pi/2).
\end{aligned}
$$

$$
\begin{aligned}
y_1 &= \cos(2\pi x) + \cos(2\pi y) \\
y_2 &= \cos(2\pi x) \cdot \cos(2\pi y) \\
y_3 &= (\cos(2\pi x) + \cos(2\pi y)) \sin 4\theta \\
y_4 &= (\cos(2\pi x) + \cos(2\pi y)) \cos 4\theta \\
y_5 &= \cos 4\theta \\
y_6 &= \sin 4\theta
\end{aligned}
$$

$$
\begin{aligned}
y_1 &= \cos(2\pi(x + y)) + \cos(2\pi(x - y)) \\
y_2 &= \cos(2\pi(x + y)) \cdot \cos(2\pi(x - y)) \\
y_3 &= \sin(2\pi x) \cdot \sin(2\pi y) \cdot \sin(2\theta) \\
y_4 &= \sin(2\pi x) \cdot \sin(2\pi y) \cdot \cos(2\theta) \\
y_5 &= \sin^2(2\pi x) \cos^2\theta + \sin^2(2\pi y) \sin^2\theta \\
y_6 &= \sin^2(2\pi x) \sin^2\theta + \sin^2(2\pi y) \cos^2\theta
\end{aligned}
$$

$$
\begin{aligned}
y_1 &= \cos(4\pi x) + \cos(4\pi y) \\
y_2 &= \cos(4\pi x) \cdot \cos(4\pi y) \\
y_3 &= \sin^2(2\pi x) + \sin^2(2\pi y) \\
y_4 &= \sin^2(2\pi x) \cdot \sin^2(2\pi y) \\
y_5 &= \sin(4\pi x) \cos\theta + \sin(4\pi y) \sin\theta \\
y_6 &= \sin(4\pi y) \cos\theta - \sin(4\pi x) \sin\theta
\end{aligned}
$$

Conclusions

- In protein crystals bodies are arranged with symmetry, but there is a hidden rigid-body motion that is important to find.
- This motion lives in a coset space (quotient of SE(3) by a discrete subgroup of crystallo-graphic symmetry operations).
- This paper characterizes this space (which is a manifold) and corresponding fundamental domains

References

G.S. Chirikjian, ``Mathematical Aspects of Molecular Replacement: I. Algebraic Properties of Motion Spaces,'' Acta. Cryst. A (2011). A67, 435–446

G.S. Chirikjian, Yan, Y., ``Mathematical Aspects of Molecular Replacement: II. Geometry of Motion Spaces,'' Acta. Cryst. A (2012). A68, 208-221.

Chirikjian, G.S., Stochastic Models, Information Theory, and Lie Groups: Volume 2 - Analytic Methods and Modern Applications, Birkhauser, Dec. 2011.

Chirikjian, G.S., Kyatkin, A.B., Engineering Applications of Noncommutative Harmonic Analysis, CRC Press, 2001.

ACKNOWLEDGMENT

This work was supported by NSF Grant RI-Medium: IIS-1162095. The author would like to thank Ms. Sajdeh Sajjadi for useful discussions.